COO-1198-900

ANOMALOUS X-RAY TRANSMISSION CHANGES IN COPPER CRYSTALS ON ELECTRON IRRADIATION AT 14 K

Bruce Stilwell Brown

Department of Physics and Materials Research Laboratory

University of Illinois, Urbana, Illinois 61801

June 1972

This technical information document is based on a thesis submitted in partial fulfillment of the requirements for the degree of Doctor of Philosophy in Physics in the Graduate College of the University of Illinois, 1972. This research was supported in part by the U. S. Atomic Energy Commission under Contract AT(11-1)-1198.

DISCLAIMER

COO-1198-900

ANOMALOUS X-RAY TRANSMISSION CHANGES IN COPPER CRYSTALS ON ELECTRON IRRADIATION AT 14 K

Bruce Stilwell Brown

Department of Physics and Materials Research Laboratory

University of Illinois, Urbana, Illinois 61801

June 1972

This technical information document is based on a thesis submitted in partial fulfillment of the requirements for the degree of Doctor of Philosophy in Physics in the Graduate College of the University of Illinois, 1972. This research was supported in part by the U. S. Atomic Energy Commission under Contract AT(11-1)-1198.

ANOMALOUS X-RAY TRANSMISSION CHANGES IN COPPER CRYSTALS ON ELECTRON IRRADIATION AT 14 K

Bruce Stilwell Brown, Ph.D.
Department of Physics
University of Illinois at Urbana-Champaign, 1972

Anomalous X-ray transmission measurements were made at 4.2 K on nearly perfect crystals before and after irradiation at 14 K with 3 MeV electrons. Simultaneous resistance measurements were taken on high purity copper wires. The measured intensity changes for (111), (222), (333), (220), (200), and (400) reflecting planes were investigated at intervals during the irradiation. Annealing studies at 22 K, 37 K, 78 K, and 295 K show X-ray intensity recoveries similar to resistance recoveries.

Resistance increases show a linear dependence with electron fluence while transmitted X-ray intensity decreases show a greater than linear dependence. Resistance changes with dose were comparable with previous data. X-ray intensity decreases appear to be greater than predicted for the estimated concentration of point defects. A second irradiation of the transmission specimen after a long room temperature anneal led to decreases in transmitted intensity which were about twice the changes seen after a similar electron fluence in the first irradiation.

ACKNOWLEDGEMENTS

The author gratefully acknowledges the constant advice and encouragement of Professor J. S. Koehler throughout the course of this investigation.

He also wishes to thank Dr. L. S. Edelheit for his patient instruction and assistance covering all aspects of this experiment. The author is indebted to Dr. F. W. Young, Jr., for the preparation of the samples.

Finally, the author wishes to thank his wife, Marlene, for her patience and understanding. Her encouragement was necessary for the successful completion of this work, and made the author's time in graduate school meaningful and enjoyable.

This research was supported in part by the U.S. Atomic Energy Commission under Contract AT(11-1)-1198.

TABLE OF CONTENTS

INTRODUCTION

Dynamical diffraction of x-rays has been the subject of considerable study[1,2] and is a powerful tool for investigating defects in nearly perfect crystals. Dislocations and large defect clusters can be photographed directly by means of x-ray transmission topography. Changes in anomalously-transmitted x-rays (Borrmann effect) resulting from defects aggregating into clusters or small dislocation loops have been studied extensively; for example, oxygen precipitated in silicon,[3] arsenic in germanium,[4] and neutron-irradiation damage in silicon,[5] germanium,[5,6] and copper.[7] Young, Baldwin, and Dederichs[8] have investigated the correlation between the decrease in anomalous x-ray transmission and defect concentrations determined by electron microscopy for fast neutron irradiated copper crystals.

Larson and Young[9] have shown that intensity changes in copper resulting from fast neutron irradiation at room temperature are consistent with the theoretically predicted intensity decreases of Dederichs[10] for the presence of defect aggregates in the form of dislocation loops. Defects introduced after electron irradiation have been investigated.[11] Long-range strain of the reflecting crystal planes has been shown to have a large effect on anomalous x-ray transmission.[12,13]

If a monochromatic x-ray beam is incident at the Bragg angle on a single crystal as shown in Figure 1 then deep in the crystal (several microns) two kinds of standing waves result. One with maximum intensity at the lattice planes, is anomalously absorbed. A second, with minimum intensity at the lattice planes, is anomalously transmitted. The intensity of the anomalously transmitted beam can be many orders of magnitude larger than

Figure 1 Geometry of the beams when anomalous transmission is occuring. When the beam emerges from the back face, it splits into two beams, one in the forward direction, and one in the diffracted direction. The energy in the beam flows along the atomic planes in the crystal.

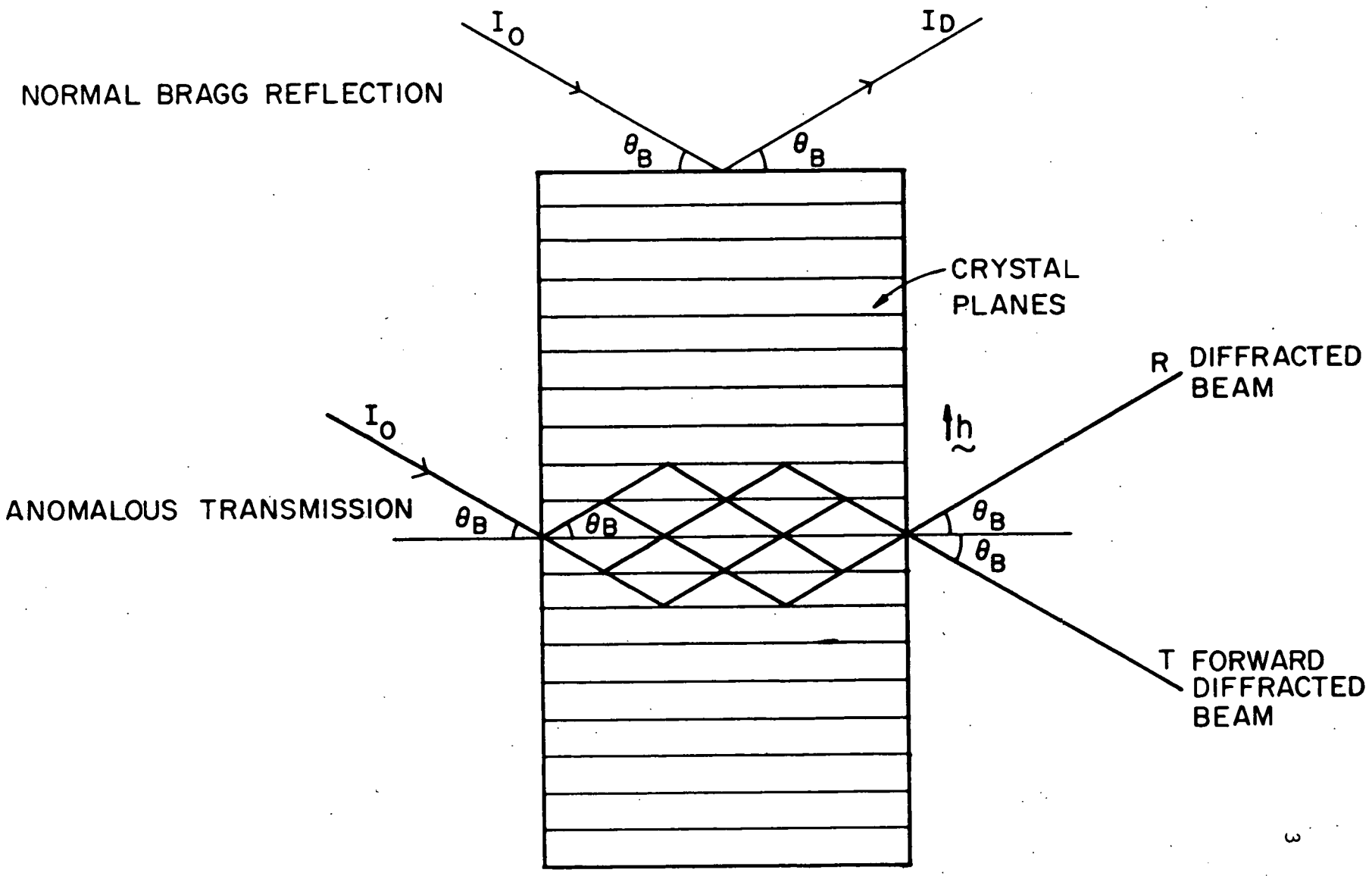
NORMAL BRAGG REFLECTION
I_O
I_D
θ_B
θ_B
CRYSTAL PLANES
R DIFFRACTED BEAM
I_O
$\vec{h}$
ANOMALOUS TRANSMISSION
θ_B
θ_B
θ_B
θ_B
T FORWARD DIFFRACTED BEAM

that of a randomly directed x-ray beam of the same wavelength. The electric field intensity distribution of the standing waves for the first, second, and third order anomalously transmitted waves is shown in Figure 2. Note that an interstitial midway between these atomic planes would absorb strongly in first and third order but would have small absorption in second order. Note also that small atomic displacements from the planes would give larger contributions to transmission changes for third order than for lower orders. In principle if the changes in anomalous transmission were measured for all diffracting planes and for all orders then if only one kind of defect was present its geometrical configuration could be determined. It was the aim of this experiment to determine the geometrical configuration of the interstitial generated by low temperature electron irradiation in copper.

The low temperature electron irradiation experiment previously performed[11] observed intensity decreases on the order of a few percent. This was the expected size of the decrease associated with the calculated concentration of isolated point defects. The large decreases in transmitted x-ray intensity found in the present experiments indicate a different behavior than that expected for isolated point defects. The observation of an enhanced intensity decrease upon redoing the experiment with the same crystals raises additional questions. The transmitted x-ray intensity changes and resistivity changes were carefully measured at intervals during the production at 14 K by electron irradiation and during subsequent annealing stages.

At present the observed changes in the anomalous x-ray transmission are not understood. Both the theory and the experimental data are being examined carefully in an attempt to determine what physical processes

Figure 2 Electric field intensity distribution for (nnn) reflections. Absorption by an atom is proportional to the electric field intensity at the atom.

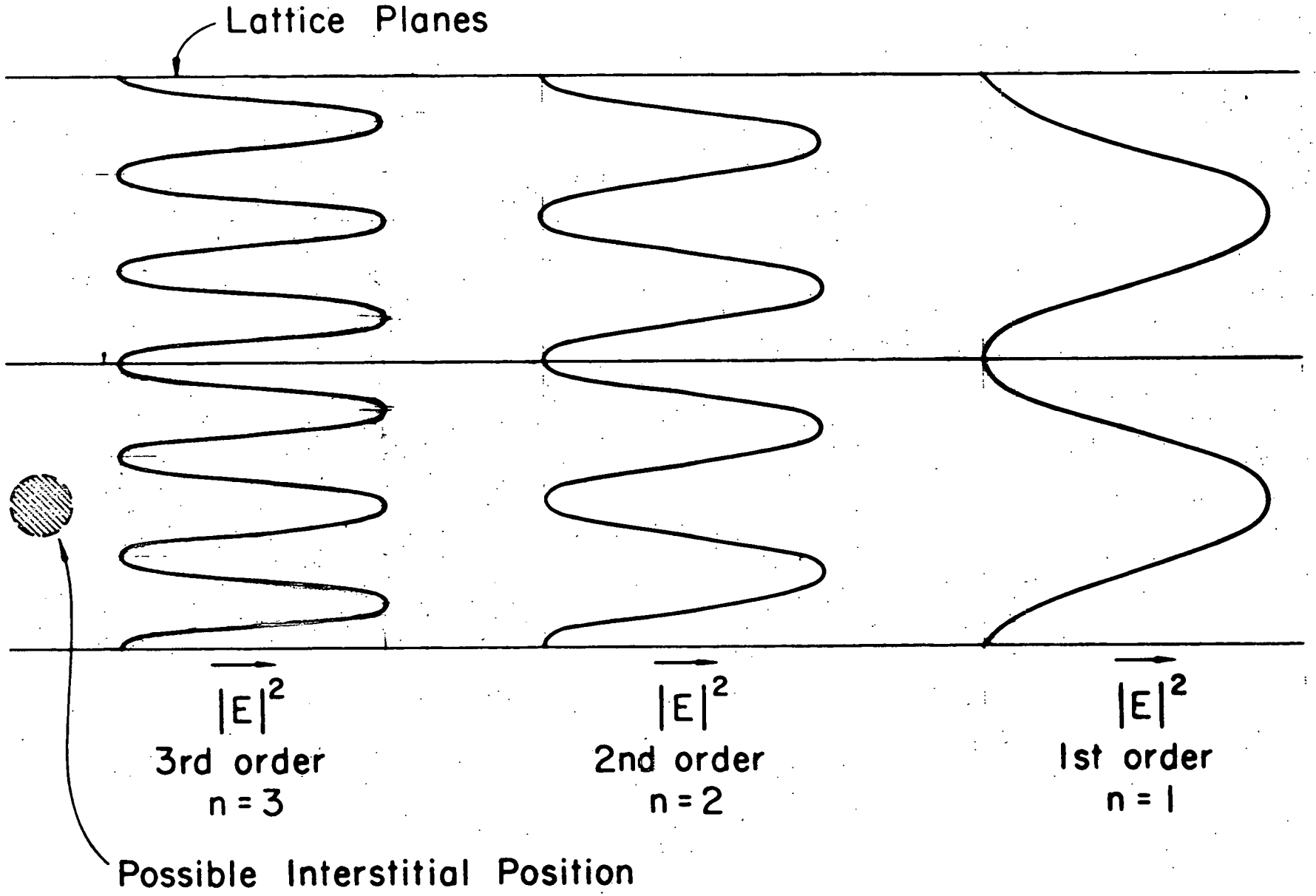
Lattice Planes
$|E|^2$
3rd order
n = 3
$|E|^2$
2nd order
n = 2
$|E|^2$
1st order
n = 1
Possible Interstitial Position

are important. The strange features of the data and the possible mechanisms responsible are described in the discussion. Several experiments aimed at clarifying the situation are suggested.

Experimental Procedure

Single crystals of 99.999^{+}% copper were prepared for Borrmann x-ray studies by Dr. F. W. Young, Jr., at the Oak Ridge National Laboratory. This preparation has been described previously.[15] A 1x1x2 cm parallelopiped was cut from the crystal by an acid saw technique.[16] This crystal was annealed at 1075 C for about two weeks to eliminate dislocations. The crystal was then irradiated with 10^{17} nvt fast neutrons at a temperature below 100 C in order to pin the remaining dislocations and thus minimize damage due to handling. It has been shown[17] that the effect on the anomalous transmission due to this irradiation is small and it is assumed that the effect remains a constant during the experiment. It has been established that copper crystals with low dislocation densities irradiated with the above neutron fluence exhibit x-ray diffraction properties equivalent to perfect crystals.[18] After irradiation, the crystal was sliced into 1x1xt cm pieces (t between .025 and .205). For our experiment two adjacent slices were chosen. The two crystals had (110) faces to within 0.5°. They were polished and electropolished[28] to eliminate surface damage.

The thickness of the crystals was determined by absolute integrated intensity measurements, and also by the relative intensities of various orders of reflection. Both crystals were 0.9 ± 0.1 mm thick. Due to the polishing process, the crystal faces were slightly convex. Thus, the crystal was thicker at the center than near the faces. Since we were interested in the change in x-ray intensity due to irradiation, any change in intensity due to thickness variations had to be minimized.

The crystals were mounted in a liquid helium cryostat that has been previously described.[11] The sample chamber is shown in Figure 3. Since anomalous transmission is very sensitive to strain, mounting was carefully performed to eliminate any mechanical strains due to differential thermal contractions upon subsequent cooling. Thus the samples were not rigidly supported, but rather placed in a copper holder with approximately 5-mil clearance on all sides. The electron irradiation added approximately one watt of power to the sample. The samples were cooled by means of about an atmosphere of helium exchange gas in the sample can which provided better convection cooling between the samples and helium reservoir. The beam current and exchange gas were adjusted to keep the samples below Stage I annealing which starts at about 16 K.

The sample temperature was measured by means of a carbon resistor glued to the sample mounting block, and all irradiation was done with $t < 14$ K. The large heat intake resulted in a high helium loss rate and required a remote control helium transfer system that permitted

Figure 3 Sectional view of the specimen chamber:

a) copper crystals to be measured;

b) 1/4" brass aperture for electron beam;

c) valve to van de Graaff;

d) ball bearing race to rotate outer chamber;

e) .010" wall inconel tubes conducting liquid helium to sample chamber;

f) liquid nitrogen temperature radiation shield;

g) 3/32" diameter stainless steel bead chain wrapped around a sprocket;

h) worm gear;

i) Barden SFR1-4R Bearing (only one shown);

j) "Xactglo" heating element to vary sample temperature;

k) worm wheel for Φ rotation;

l) cut outs in sample mount used to locate the crystal position;

m) copper posts used to align the electrom beam with respect to the sample;

n) 3/16" copper shield which can be raised from above to shield the lower copper crystal from electron irradiation;

o) copper fins used to cool helium exchange gas;

p) 8-mil copper resistivity wires.

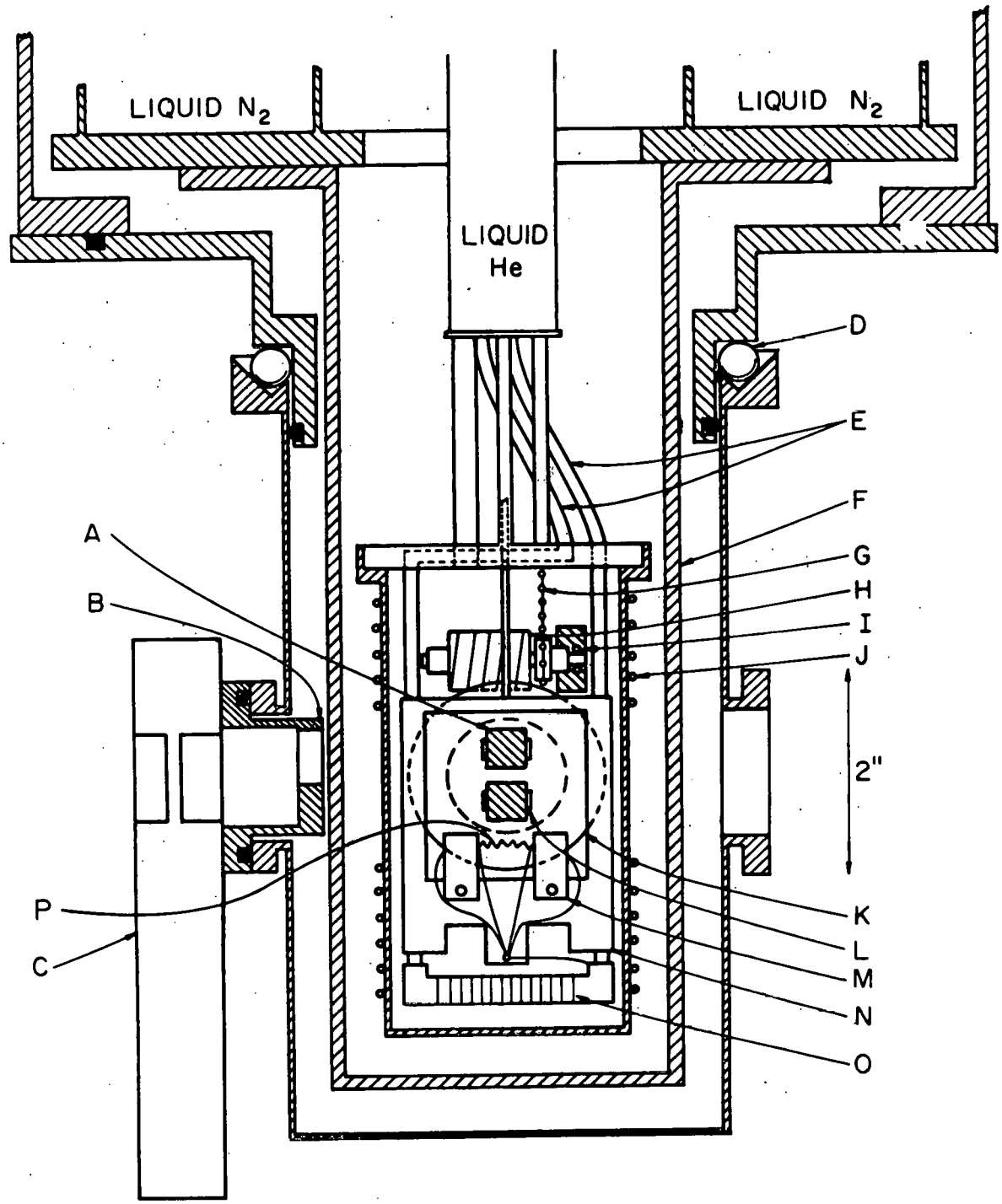
LIQUID N_2
LIQUID N_2
LIQUID
He
D
E
F
G
H
I
J
A
B
2"
P
C
K
L
M
N
O

the transferring of liquid helium without discontinuing the electron irradiation. The cryostat design allowed two translational degrees of freedom ($\pm$ .01 mm) and two rotational degrees of freedom. The Bragg angle could be set to within 1 sec of arc; rotation about a normal to the crystal face was accurate to $\pm$ .05°.

As a check on the stability of the x-ray production and detection apparatus, the experiment was performed using two copper crystals. One sample was shielded from the electrons during irradiation and a movable shield was lowered to expose both samples for the x-ray measurements. In this way the change in x-ray intensity on the irradiated sample indicated the effect of the electron irradiation and the change in x-ray intensity on the shielded sample indicated any drift in the x-ray apparatus. By comparing the x-ray intensity of the irradiated sample to that of the unirradiated sample the drift effect could be eliminated. For all measurements the drift effect was small, generally less than 1% in a month.

The resistivity samples were 8-mil diameter Cominco American 99.999% pure copper wires. Two wires were used, one in front of the x-ray crystals and one behind. The wires were bent in the manner indicated in Figure 1 to enable mechanical strains from differential thermal contractions upon cooling to be accommodated without any sample elongation. High purity copper leads were spot welded to the wires. The wires were carefully cleaned with benzene, methanol, HNO_3, and distilled water and were annealed at 800 C for three hours in a vacuum of 5×10^{-6} torr. A side view of the final mounting and the movable shield is shown in Figure 4. This arrangement allowed the wires to be

Figure 4 Rotating sample holder:

a) 8-mil copper resistivity wires mounted in nylon bushings;

b) copper crystals which are free to move in the mount;

c) .005" Be-Cu strip to prevent sample from falling out;

d) 1/16" thick copper mount;

e) worm wheel which is turned by the worm gear (f);

g) outer bearing clamp;

h) Miniature Precision Bearing Company 3TK1 bearing with stainless steel race and balls with teflon spacer slugs;

i) inner bearing clamp;

j) electron shield in "up" position for electron irradiation.

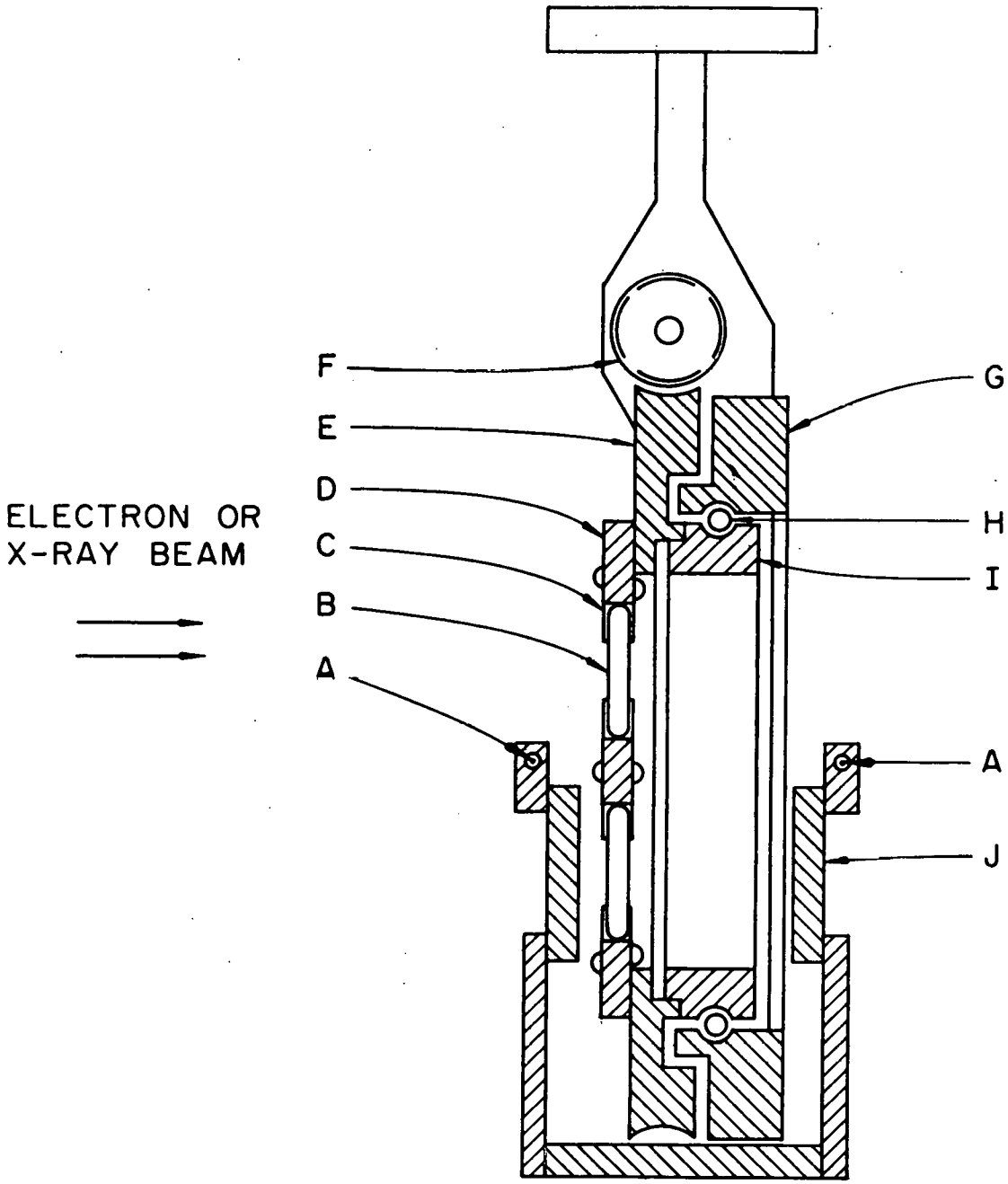
ELECTRON OR
X-RAY BEAM
F
E
D
C
B
A
G
H
I
A
J

raised into the electron beam for irradiation and lowered to allow x-ray irradiation with the wires well below the lower x-ray sample. The result of preparation, annealing, and mounting was a residual resistivity of the mounted copper wires of 1.60×10^{-9} ohm-cm at 4.2 K, a room temperature to helium temperature resistivity ratio of 970.

Specimen resistance was measured potentiometrically using a Rubicon 6-Dial Thermofree Potentiometer and current-emf switching arrangement to correct for thermal emf's. The current through the specimen during measurement was 1.0 ampere and was regulated to 1 part in 10^5. No change in residual resistivity was observed for controlled currents in the range from .1 ampere to 1.5 ampere. At 1.0 ampere no change in resistivity was observed for different shield positions or after many raisings and lowerings of the shield. This indicated no cold working was being performed on the samples by moving the shield. The precision of a typical series of resistance measurements was $\pm .2 \times 10^{-7}$ ohm, corresponding to a resistivity uncertainty of $\pm 4 \times 10^{-12}$ Ω-cm.

For resistance measurements taken with samples of small dimensions and at helium temperature, the mean free path for the conduction electrons becomes on the order of the sample dimensions and surface contributions must be considered. The surface contribution depends on the mean free path of the conduction electrons and is, therefore, not constant during irradiation as the resistivity changes with fluence. The surface contribution calculations were taken directly from Sondheimer's theory assuming completely diffuse scattering.[19] The result for the pre-irradiated .008-mil copper wire at 4.2 K is to reduce the bulk resistivity by about 13%. The bulk resistivity change from pre-irradi-

ation to full irradiation increases less than 0.3% from the uncorrected resistivity change values and will not be included in the results.

The x-ray power supply was a GE XRD-6 unit with a constant potential assembly and voltage stabilizer to minimize power fluctuations. A molybdenum target x-ray tube was used, and the sample was adjusted to anomalously transmit x-rays.

No monochromator was used in the system. This precluded making absolute integrated intensity measurements. However, since the primary interest was the change of the x-ray intensity, an absolute integrated intensity determination was not necessary. Furthermore, the monochromators tested introduced nonuniformities in the x-ray beam that led to variations in the measurements beyond our required precision.

The intensity measurements were made using a NaI(Tl) detector. A single-channel analyzer discriminated against $\lambda/2$ radiation and a 0.006-in. aluminum filter in front of the detector reduced the number of low-energy x-rays to a negligible contribution. The amplification and pulse-height analysis components of the counting system were enclosed in a constant temperature cabinet ($\pm$ 1 C) to minimize the temperature effects of these components. Counts of Fe^{55} decay up to 10^7 were consistent within statistics (~0.03%) over periods of days.

Measurements were made at two locations on the unirradiated reference crystal (LOC 1 and 2) and two locations on the irradiated crystal (LOC 3 and 4). Because of sample-thickness variations, the same locations were always used and were relocated to $\pm$ 0.03 mm. The x-ray-beam diameter at the crystal was 2 mm. All intensity measurements were made by maximizing the counting intensity for MoK_α x-rays. This peak intensity

was then measured. Since no monochromator was used, some x-rays other than MoK_α are transmitted; however, their number is small and the same for both unirradiated and irradiated crystals. At the peak the change in counting intensity from the peak value to 99% of the peak value was smooth and corresponded to a change in θ of about 200". The location of the peak was determined to 8" corresponding to about 0.02% change in intensity.

The effect of long-range strains on the anomalous transmission intensity was minimized by using the average intensity of the (hkl) and $(\bar{h}\bar{k}\bar{l})$ reflections. This has been justified[12,13] and will be mentioned in the discussion.

The experiment consisted of two runs with a long room temperature anneal between them. Run I consisted of measurements before irradiation, after irradiating with $.42 \times 10^{18}$ e/cm^2 and after $.83 \times 10^{18}$ e/cm^2. Resistivity and x-ray measurements were taken after annealing the samples at 22 K for two hours, after annealing at 37.2 K for one hour, after annealing at 78 K for 24 hours, and after annealing at 295 K for 24 hours. All measurements were made at liquid-helium temperature (4.2 K). The first three orders of the (111) planes, the first two orders of the (200) planes and the first order of the (220) planes were measured. Pre-irradiation data were not available for the two orders of the (200) planes. To check reproducibility the measurements were made twice after the irradiation of $.42 \times 10^{18}$ e/cm^2 and the results agreed within experimental error.

The samples were kept in vacuum at room temperature for three months after Run I. Run II used the same resistance samples and the same

measurement locations on the x-ray crystals. Run II consisted of measurements before irradiation and after fluences of $.10 \times 10^{18}$ e/cm^2, $.21 \times 10^{18}$ e/cm^2, and $.42 \times 10^{18}$ e/cm^2. The first three orders of the (111) planes and the first order of the (220) planes were measured. Brief measurements were taken after annealing to 78 K for 24 hours.

A High Voltage Engineering van de Graaff accelerator was the source of the irradiating electrons. The (3.0 ± 0.1)-MeV electron-beam current was 0.35 A/cm^2, and the sample temperature during irradiation was kept below 14 K. The total fluence of $.83 \times 10^{18}$ e/cm^2 in Run I required about 140 hours irradiation time. In Run I after a fluence of 0.21×10^{18} e/cm^2 and 0.63×10^{18} e/cm^2 and in Run II after a fluence of 0.05×10^{18} e/cm^2, 0.15×10^{18} e/cm^2, and 0.32×10^{18} e/cm^2; the cryostat was rotated 180° so that half the fluence was incident on the opposite face of the crystal for each dose. This was done to reduce the strains in the crystal due to defect concentration gradients. Since the electrons lost about 1.0 MeV in traversing the crystal, the total displacement cross section (including secondary displacements) went from about 127 barns at the entering face to about 107 barns at the exit face assuming a displacement threshold energy of 22 eV.[20] Thus, the concentration of defects was less at the back surface of the crystal than at the front surface. This was partially compensated for by the Yang correction[14] because the path length (and hence the damage production) was larger near the back face due to multiple scattering resulting in increased path length. Because of the neutron hardening, the strain due to the defect concentration gradient will be elastic for reasonably small concentrations. By irradiating with half the fluence incident on one surface and half the

fluence incident on the opposite surface, the concentration gradients were made smaller. Calculations show that the defect concentration was a maximum at the center of the crystal, and the difference from the center to either surface was less than 3%. The effect of the concentration gradient appears to be small.

As a result of rotating the cryostat by 180°, the resistance wires (which are mounted in front of and behind the crystals) are exposed to only half the total fluence of the crystals. The wires are about 1 cm from the face of the crystal and multiple scattering of the electrons in traversing the crystal effectively defocuses the beam to the point that the sample behind the crystal sees little irradiation. This was verified experimentally by observing the resistivity change of the wire in front and in back. In all cases the resistivity change of the back wire was zero to within experimental error.

Experimental Results

The intensity of the anomalously transmitted x-rays was normalized by taking the ratio of the count rate for the irradiated crystal (LOC 3 and 4) to the count rate at one location on the unirradiated crystal (LOC 1 and 2). The percentage change of this ratio as a function of irradiation fluence and subsequent annealing temperature for Run I is listed in Table 1 and shown in Figures 5-8. $\Delta I/I_o$ represents the percentage decrease of the x-ray intensity.

$$\frac{\Delta I}{I_o} = \frac{I_{\text{BEFORE IRRAD}} - I_{\text{AFTER IRRAD}}}{I_{\text{BEFORE IRRAD}}} = \frac{I_o - I}{I_o} \quad .$$

The values plotted are the changes of the averages of the (hkl) and $(\bar{h}\bar{k}\bar{l})$ reflections. The difference in intensity changes for Run I and Run II

Table 1

Percentage Decrease in Transmitted X-ray Intensity $\frac{\Delta I}{I_o}$

Reflecting planes	RUN I After 1/2 flux	After total flux	After 22 K Anneal	After 37 K Anneal	After 77 K Anneal	After 295 K Anneal
111-1	.8	3.4	3.4	.9	.3	.2
111-2	5.8	23.2	23.0	6.8	.6	.2
111-3	22.8	65.7	65.6	24.3	4.4	.1
220-1	5.4	19.4	19.2	6.0	.2	.1
200-1	--	.4	--	--	--	.2
200-2	--	1.6	--	--	--	.4

Reflecting planes	RUN II After 1/8 flux	After 1/4 flux	After 1/2 flux	After 77 K Anneal
111-1	--	--	1.5	--
111-2	.5	2.9	11.8	--
111-3	2.9	13.9	40.8	4
220-1	.4	2.4	9.6	--

Figure 5 Decrease in anomalously transmitted intensity for the (111) reflection for Run I. The left side of the figure shows the intensity decrease vs electron fluence. The right side shows the intensity decrease vs annealing temperature.

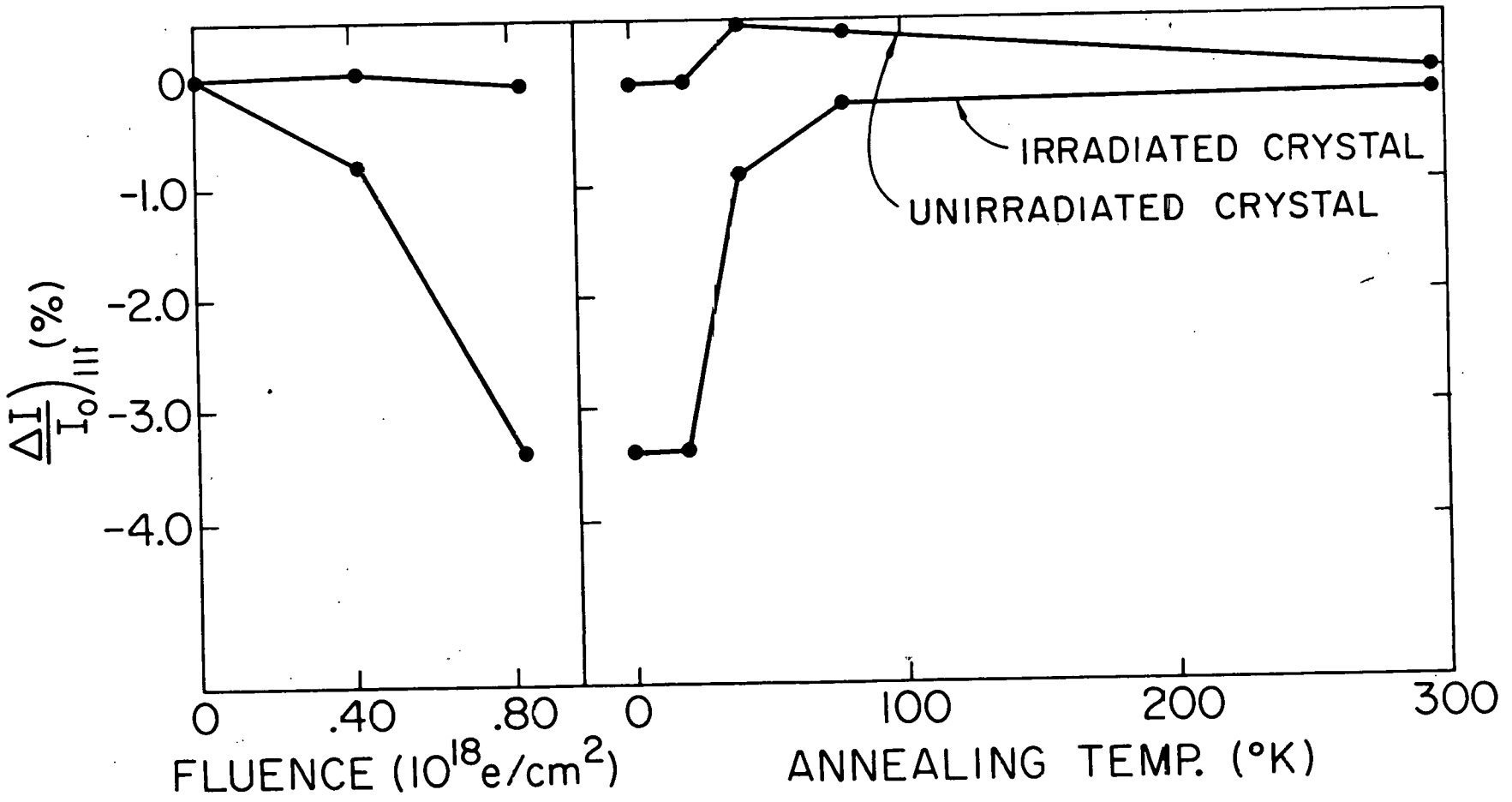
0
-1.0
-2.0
-3.0
-4.0
$\frac{\Delta I}{I_o})_{III}$ (%)
0
.40
.80
FLUENCE (10^{18}e/cm^2)
0
100
200
300
ANNEALING TEMP. (°K)
IRRADIATED CRYSTAL
UNIRRADIATED CRYSTAL

Figure 6 Decrease in anomalously transmitted intensity for the (222) reflection for Run I. The left side of the figure shows the intensity decrease vs electron fluence. The right side shows the the intensity decrease vs annealing temperature.

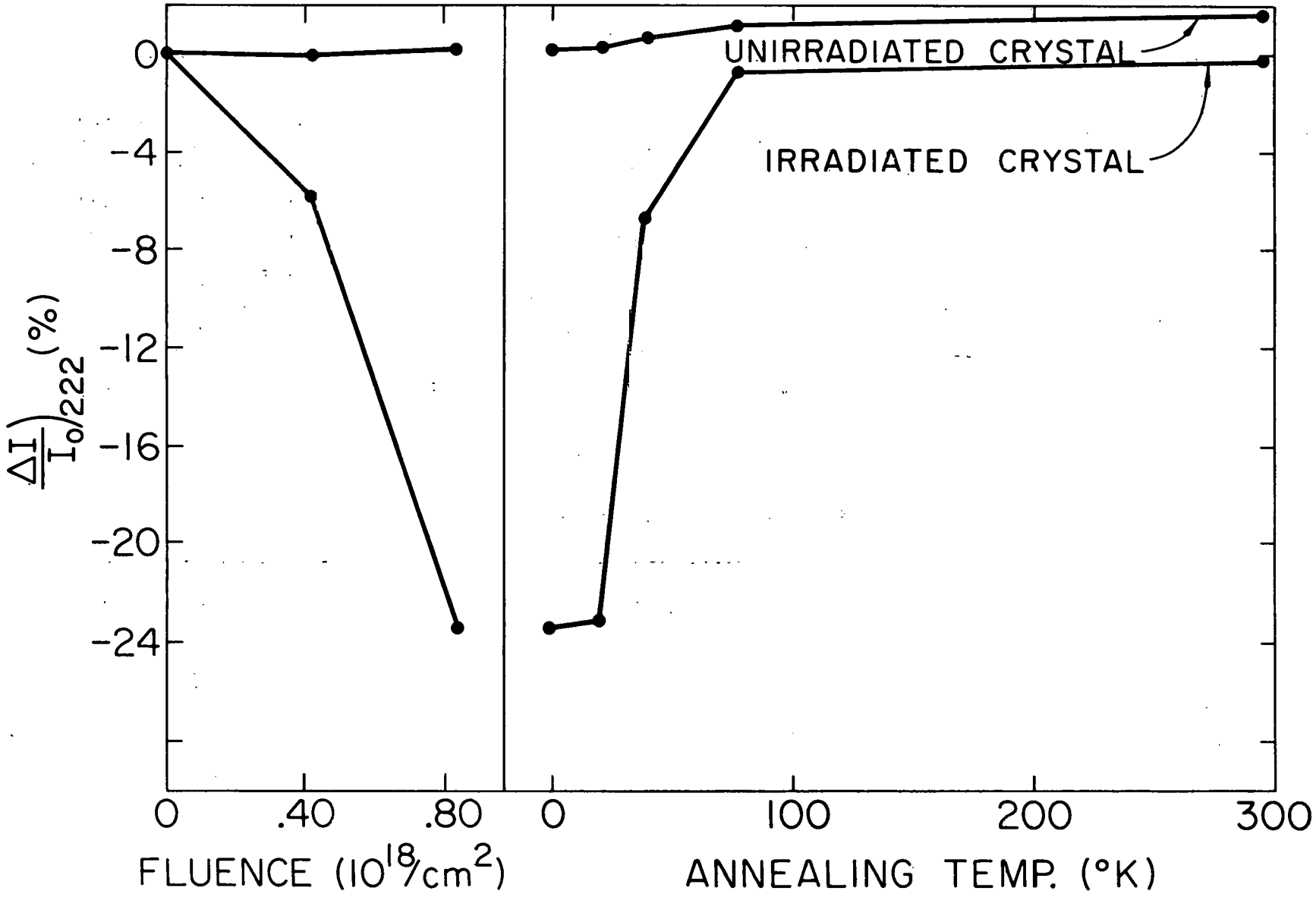
0
-4
-8
-12
-16
-20
-24
$\frac{\Delta I}{I_0}_{222}$ (%)
UNIRRADIATED CRYSTAL
IRRADIATED CRYSTAL
0
.40
.80
FLUENCE (10^{18}/cm^2)
0
100
200
300
ANNEALING TEMP. (°K)

Figure 7 Decrease in anomalously transmitted intensity for the (333) reflection for Run I. The left side of the figure shows the intensity decrease vs electron fluence. The right side shows the intensity decrease vs annealing temperature.

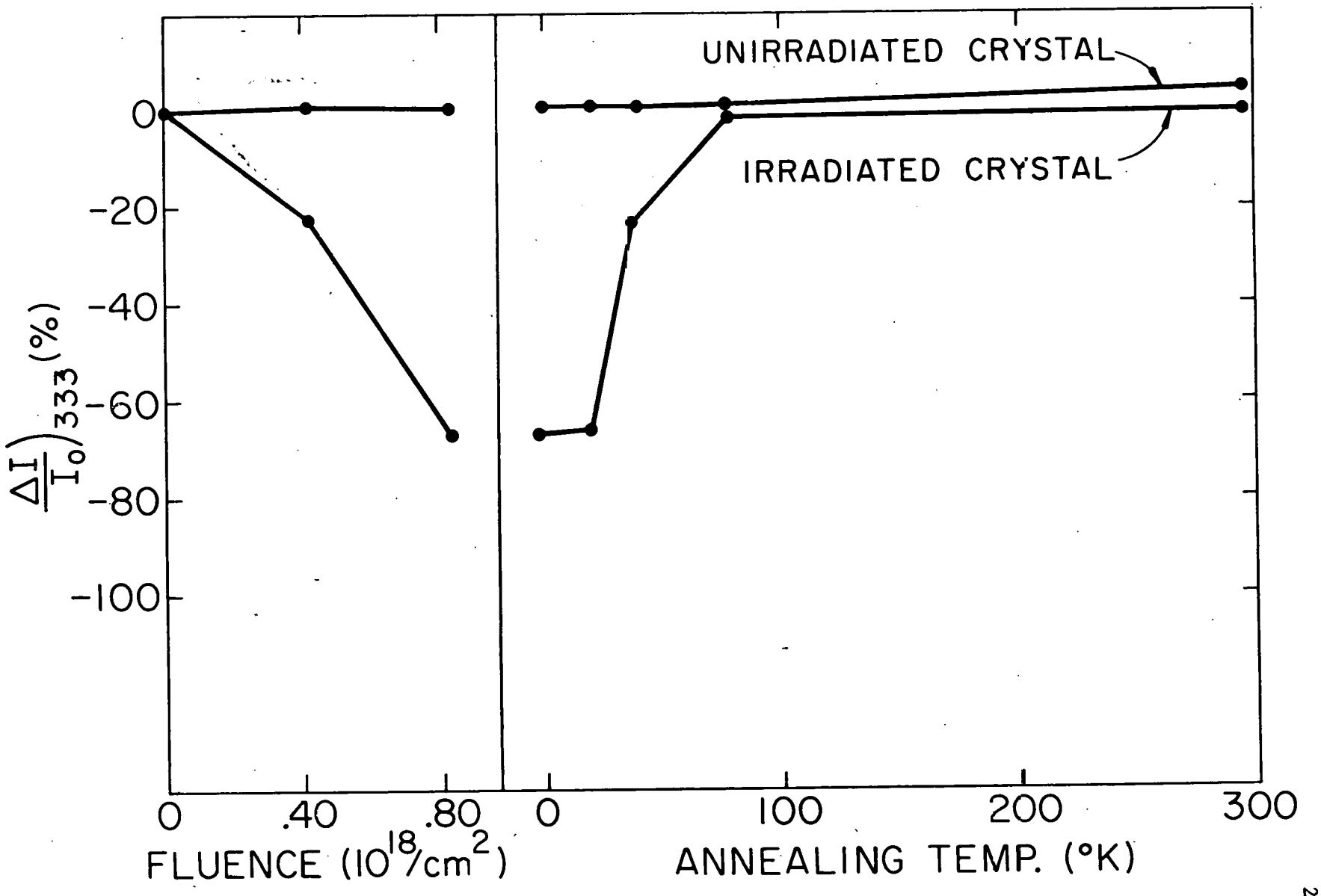
UNIRRADIATED CRYSTAL
IRRADIATED CRYSTAL
0
-20
-40
-60
-80
-100
$\frac{\Delta I}{I_0})_{333}$ (%)
0
.40
.80
FLUENCE (10^{18}/cm^2)
0
100
200
300
ANNEALING TEMP. (°K)

Figure 8 Decrease in anomalously transmitted intensity for the (220) reflection for Run I. The left side of the figure shows the intensity decrease vs electron fluence. The right side shows the intensity decrease vs annealing temperature.

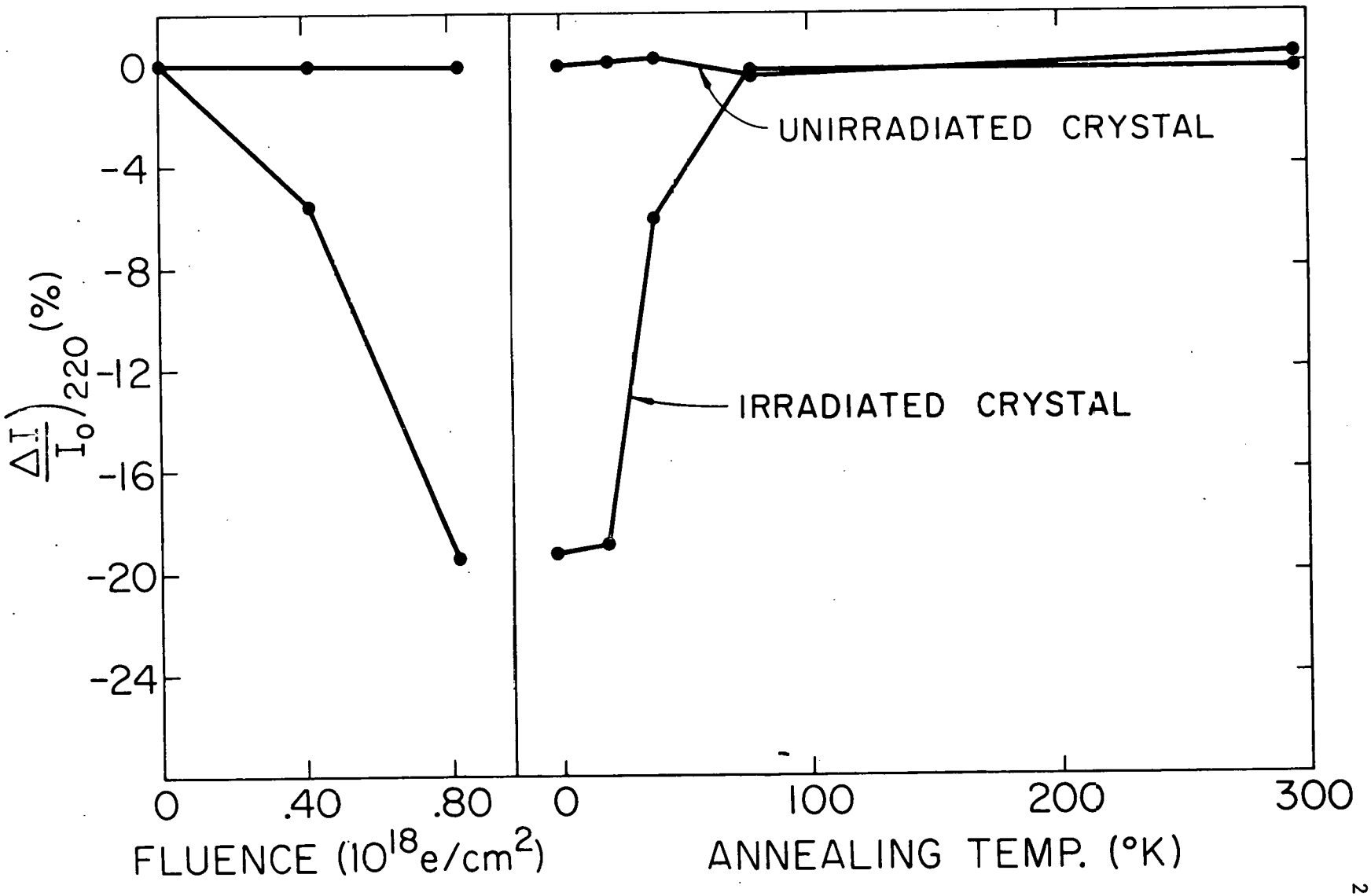
0
-4
-8
-12
-16
-20
-24
$\frac{\Delta I}{I_o})_{220}$ (%)
UNIRRADIATED CRYSTAL
IRRADIATED CRYSTAL
0
.40
.80
FLUENCE (10^{18}e/cm^2)
0
100
200
300
ANNEALING TEMP. (°K)

is shown in Figures 9-12. The resistivity changes with irradiation and annealing for both runs are shown in Figure 13. A more detailed listing of the data is in the APPENDIX.

There were a number of possible sources of error in the x-ray measurements: failure to set the crystal exactly at the maximum of the Bragg peak, fluctuations of x-ray tube and detection apparatus, counting statistics, and error in reproducing the same crystal position. Considerable effort was expended to minimize all of these problems and a result of that effort can be seen by inspecting the ratio of the two locations on the unirradiated crystal. This is indicated as LOC 2 in the figures, and the small changes shown there give an estimate of the accuracy. Intensity measurements at LOC 3 and LOC 4 indicate that the crystal thickness at LOC 3 is about 1% greater than at LOC 4. The intensity change after irradiation is proportional to the sample thickness and LOC 3 should, therefore, exhibit a slightly larger $\Delta I/I_o$ than LOC 4. This is seen to be the case for all planes for both runs. The similar behavior of LOC 3 and LOC 4 after this small (about 1%) correction is another indication of the approximate error size. The discussion in the next section of the overall behavior shows that these errors of at most a few percent are negligible.

The resistivity data is listed in Table 2. Both runs show a resistivity increase approximately linear with fluence. The fluence was determined by a Faraday cup arrangement with the entire cryostat acting as a cup. All electrons that went through a 3/8" brass aperature 2" in front of the sample were collected. The linearity of the resistivity change is easily observed in Figure 13. This acts as a check on our fluence measurement.

Table 2

Resistivity Increase From Unirradiated Values (10^{-10} Ωcm)

	RUN I					
	After 1/4 flux	After 1/2 flux	After 22 K Anneal	After 37 K Anneal	After 77 K Anneal	After 295 K Anneal
Sample 1	19.80	43.20	40.10	20.69	6.51	1.31
Sample 2	15.39	36.61	35.53	17.22	5.21	.81

	RUN II			
	After 1/16 flux	After 1/8 flux	After 1/4 flux	After 77 K Anneal
Sample 1	6.23	11.59	22.77	3.43
Sample 2	6.73	11.91	23.77	3.33

Figure 9 Decrease in anomalously transmitted intensity for the (222) reflection for both runs. LOC 2 is on the unirradiated crystal, LOC 3 and LOC 4 are on the irradiated crystal.

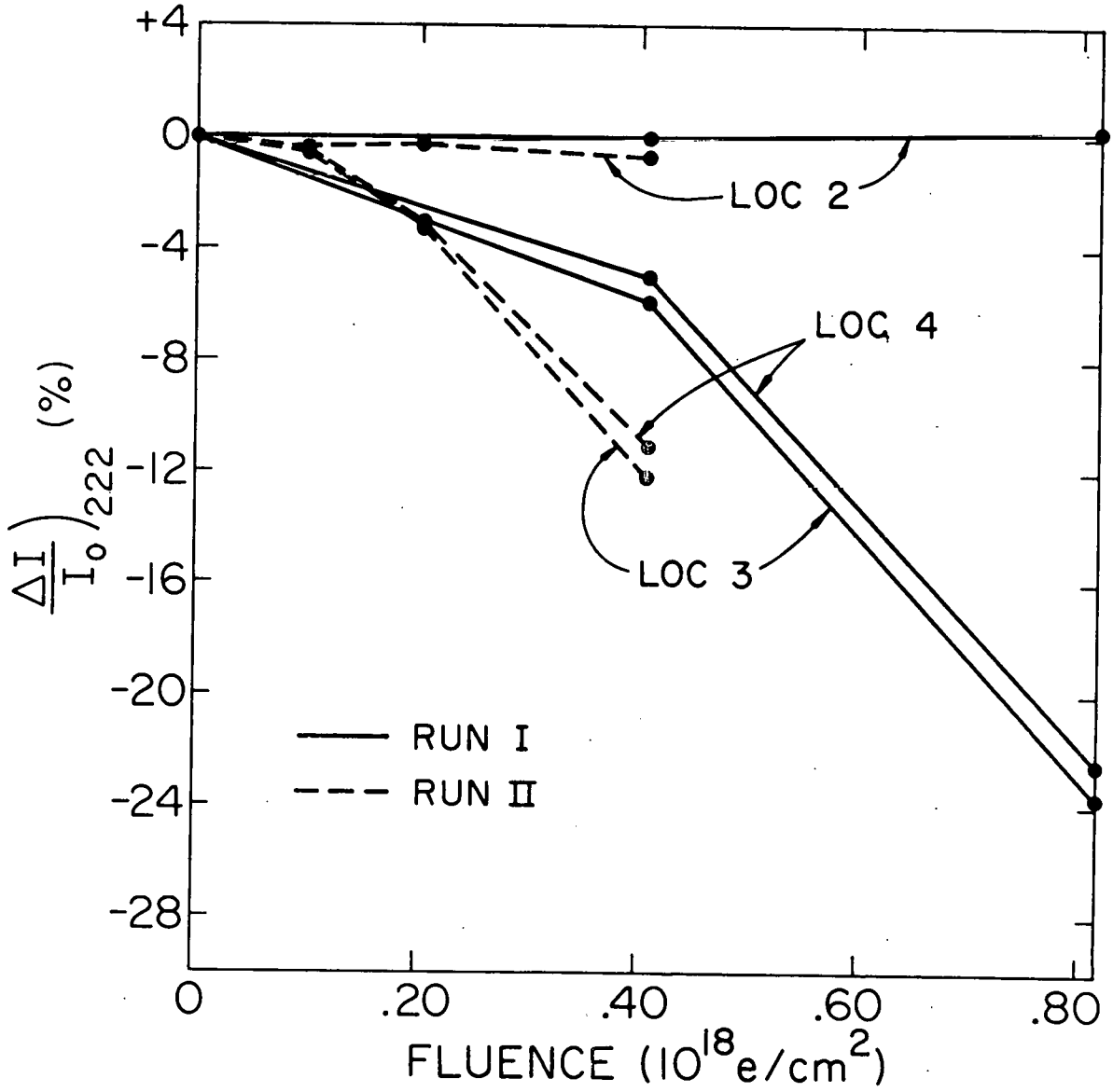
+4
0
-4
-8
-12
-16
-20
-24
-28
(%)
$\frac{\Delta I}{I_o})_{222}$
LOC 2
LOC 4
LOC 3
RUN I
RUN II
0
.20
.40
.60
.80
FLUENCE (10^{18}e/cm^2)

Figure 10 Decrease in anomalously transmitted intensity for the (333) reflection for both runs. LOC 2 is on the unirradiated crystal, LOC 3 and LOC 4 are on the irradiated crystal.

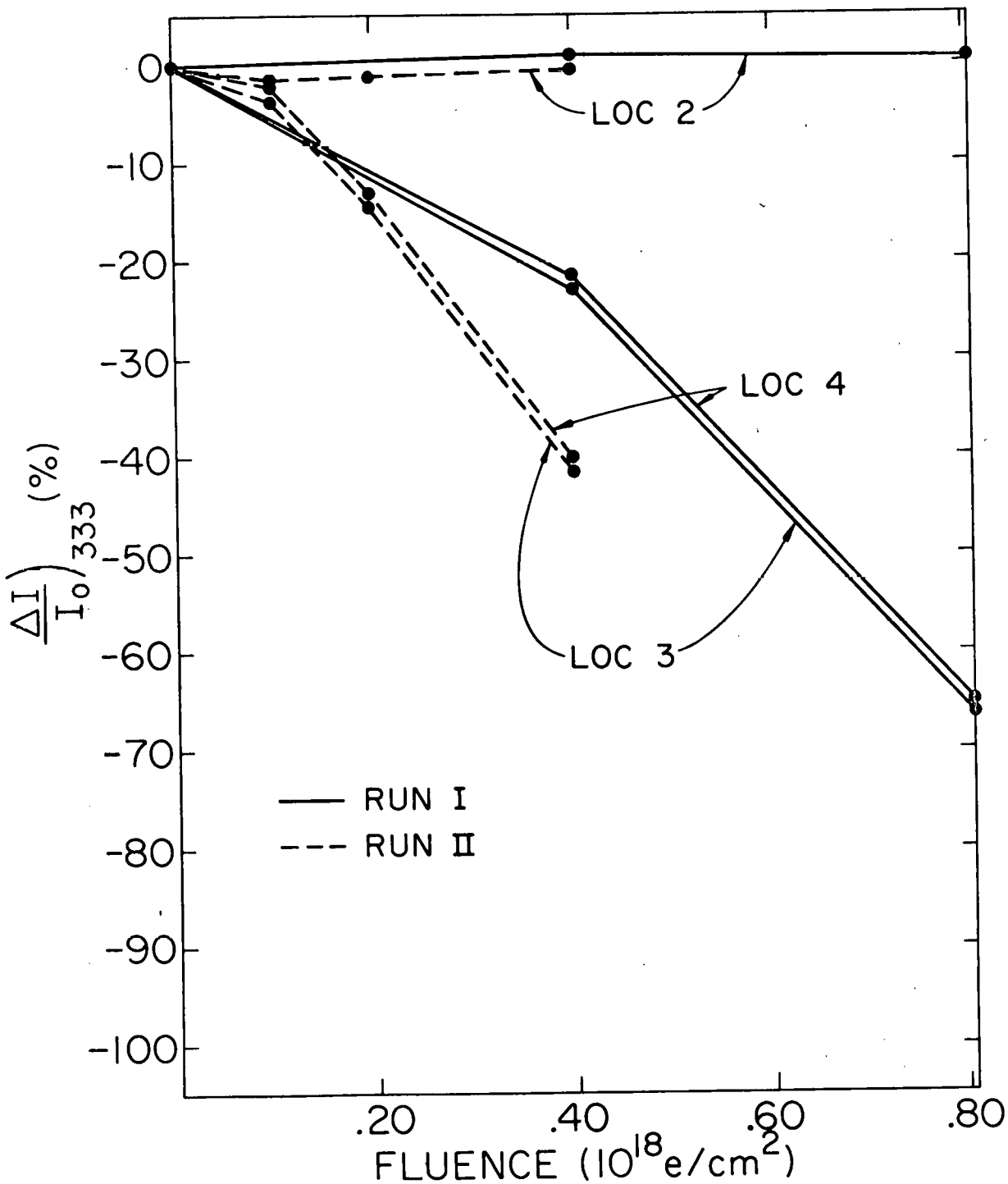
0
-10
-20
-30
-40
-50
-60
-70
-80
-90
-100
$\frac{\Delta I}{I_o}\Big)_{333}$ (%)
LOC 2
LOC 4
LOC 3
RUN I
RUN II
.20
.40
.60
.80
FLUENCE (10^{18}e/cm^2)

Figure 11 Decrease in anomalously transmitted intensity for the (220) reflection for both runs. LOC 2 is on the unirradiated crystal, LOC 3 and LOC 4 are on the irradiated crystal.

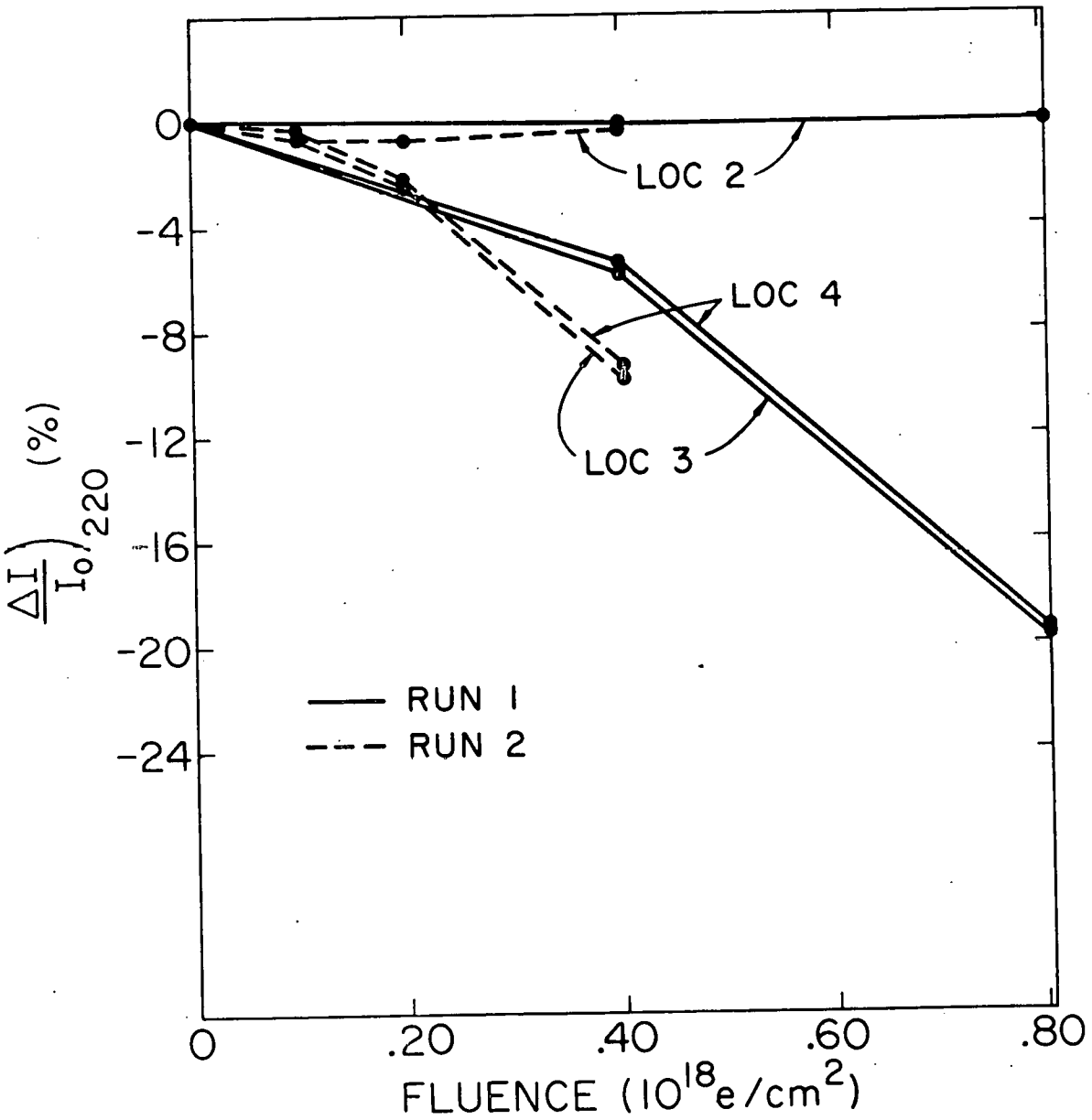
0
-4
-8
-12
-16
-20
-24
$\frac{\Delta I}{I_o}_{220}$ (%)
LOC 2
LOC 4
LOC 3
RUN 1
RUN 2
0
.20
.40
.60
.80
FLUENCE (10^{18}e/cm^2)

Figure 12. Comparison of anomalously transmitted intensity decreases for (222), (333), and (220) planes for both runs.

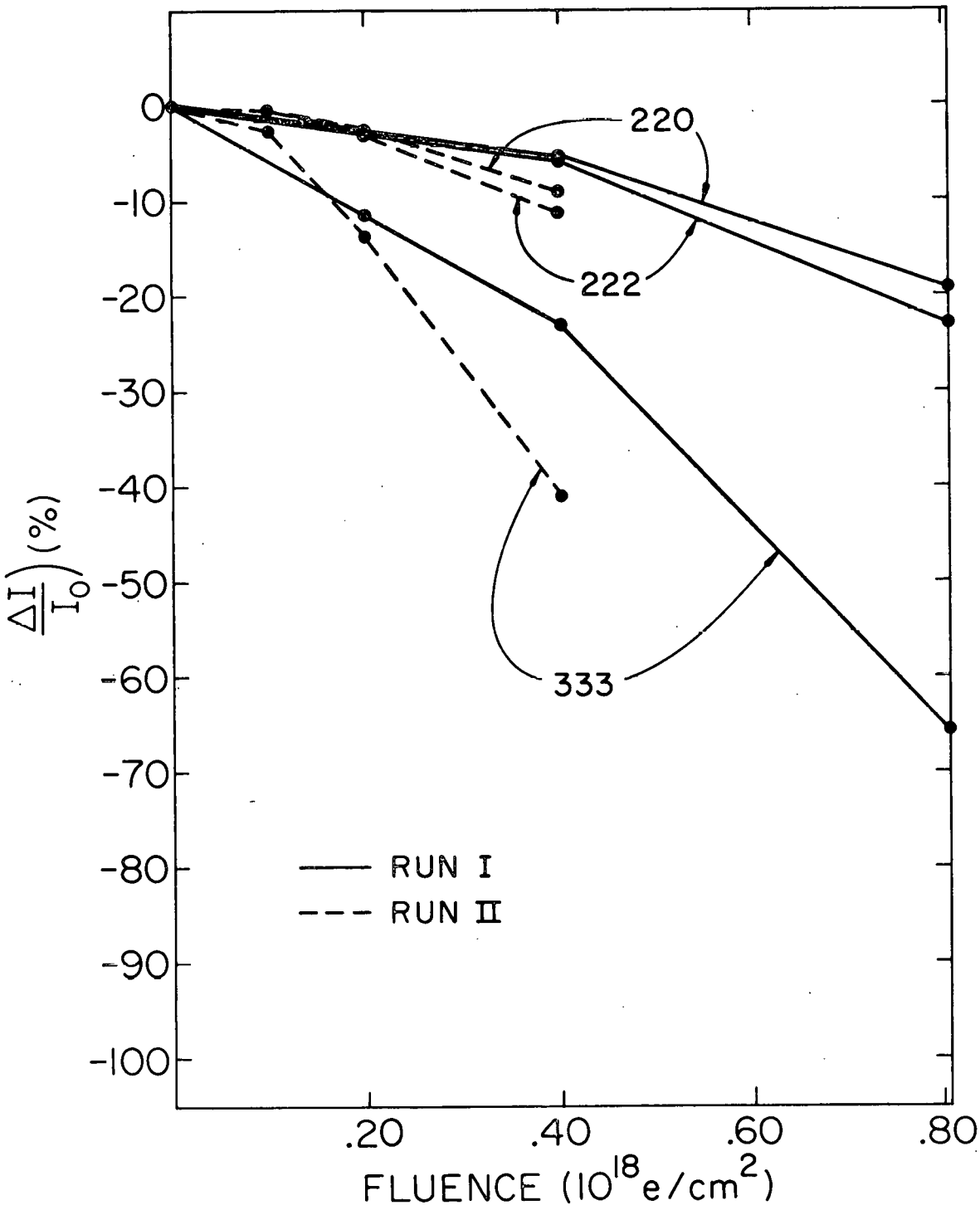
0
-10
-20
-30
-40
-50
-60
-70
-80
-90
-100
$\frac{\Delta I}{I_0}$ (%)
220
222
333
RUN I
RUN II
.20
.40
.60
.80
FLUENCE (10^{18} e/cm^2)

Figure 13 Resistivity change for both wires for both runs. The left side of the figure shows the resistivity increase vs electron fluence. The right side shows the resistivity increase vs annealing temperature.

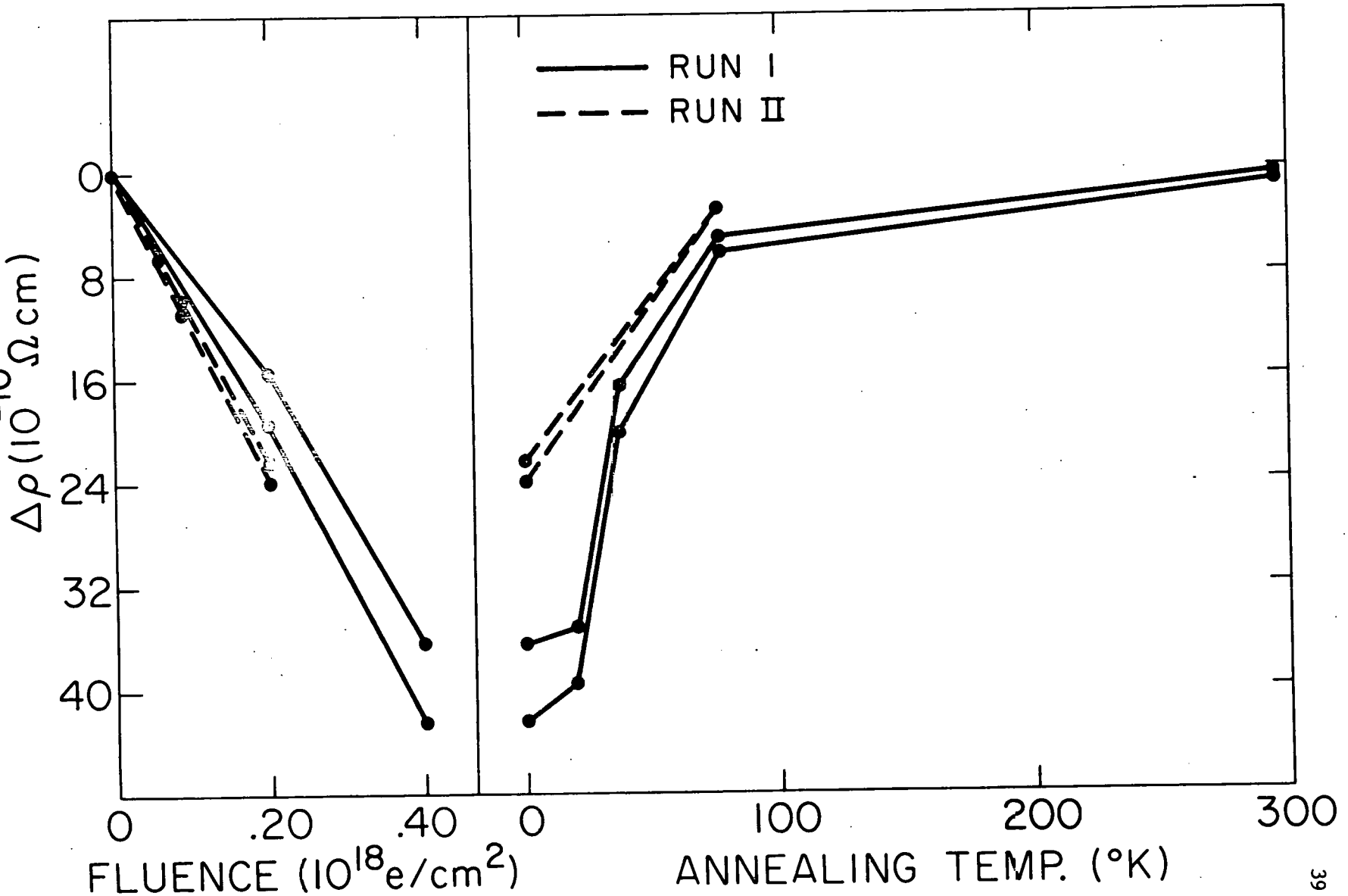
RUN I
RUN II
0
8
16
24
32
40
$\Delta\rho\,(10^{-10}\,\Omega\,cm)$
0
.20
.40
FLUENCE (10^{18}e/cm^2)
0
100
200
300
ANNEALING TEMP. (°K)

The 22 K annealing stage was investigated to see if annealing to the temperature of a previous irradiation[11] would have any effect. Very little recovery was observed. The 37 K annealing stage was selected in an attempt to separate Stages Ib, c, d from Stage Ie. The annealing temperature and time were selected such that less than 1% of Stage Ie would anneal. The uncorrelated long-range motion of Stage Ie is described by a second order kinetic rate equation as presented in Granato and Nilan.[21] The liquid nitrogen annealing stage (78 K) was investigated to see the effect of full Stage I annealing. Finally, a room temperature anneal was taken to observe any additional recovery. The percentage annealed in each stage is listed in Table 3, and the resistivity data agree very well with previous annealing studies.[14,22] The resistivity recovery is compared with the x-ray intensity recovery for the (333) planes in Figure 14. The room temperature resistivity was calculated using the value 1.55 μΩ-cm at 0 C and a temperature coefficient of 4.33×10^{-3}/degree for the resistivity of copper.[23] Values of the residual resistivity and resistivity changes were found by calculating the ratio of room temperature to low temperature resistances. Three of the four data show a similar production rate of 22.8×10^{-10} Ω-cm for a fluence of $.21 \times 10^{18}$ e/cm^2 with the fourth value about 20% lower. The purpose of the resistivity measurement was to inspect such aspects as uniformity of electron beam over the long irradiation times, effectiveness of keeping the temperature below point defect migration temperatures, and the effect of subsequent anneals. The data of the resistance measurements agree with previous data of Corbett et al.[22] sufficiently well to remove most questions on beam uniformity, temperature control, and annealing effects.

Table 3

X-Ray Intensity and Resistivity Recovery After Annealing

	RUN I				RUN II
Reflecting Planes	After 22 K	After 37 K	After 77 K	After 295 K	After 77 K
111-1	0%	74%	91%	94%	--
111-2	1%	71%	97%	99%	--
111-3	1%	63%	93%	99%	92%
220-1	1%	69%	98%	99%	--
Resistivity					
Sample 1	7%	52%	85%	97%	85%
Sample 2	3%	53%	86%	98%	86%

Figure 14 Comparison of resistivity change and anomalous transmission decrease for (333) planes. The left side shows the changes vs electron fluence. The right side shows the changes vs annealing temperature.

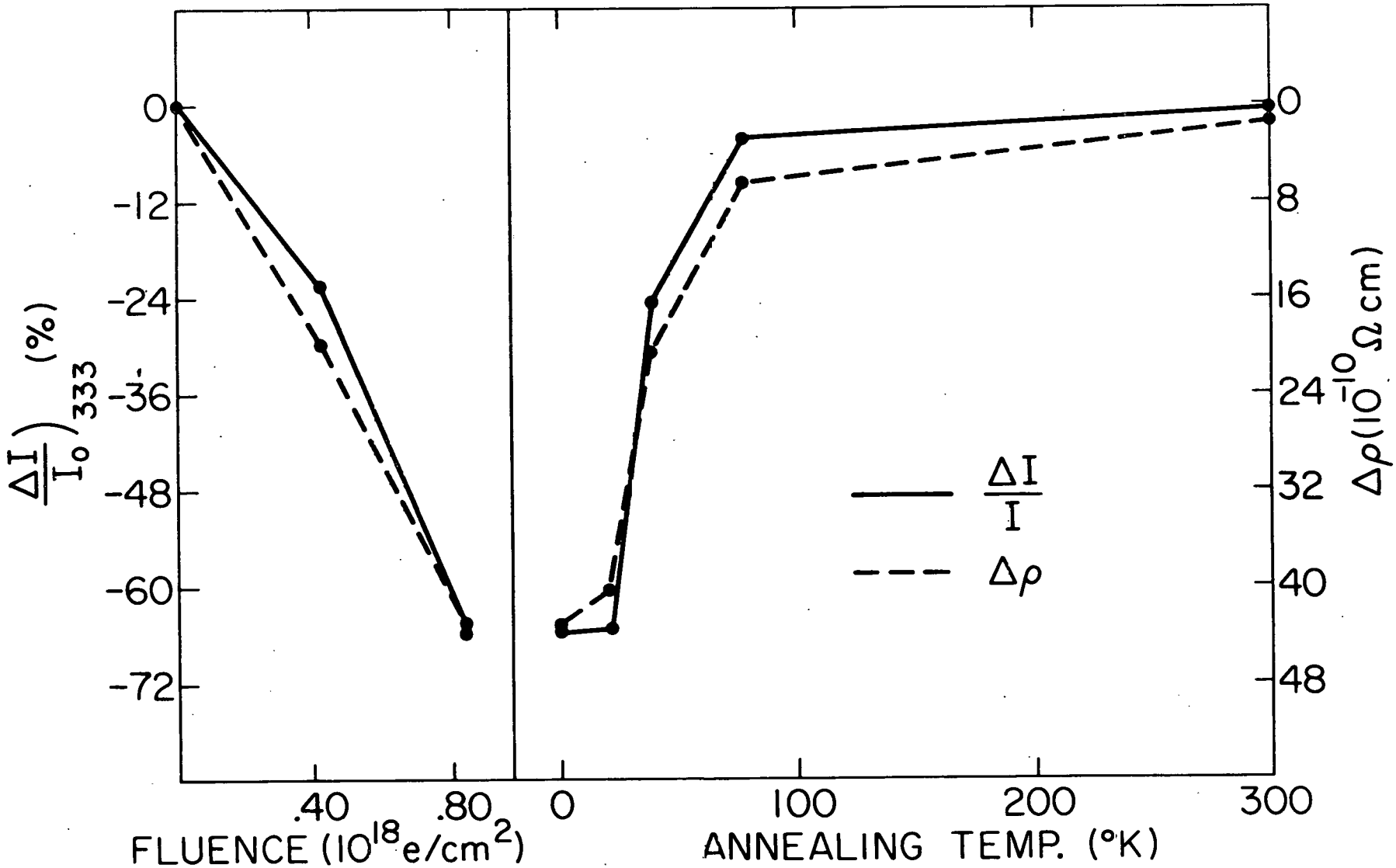
0
-12
-24
-36
-48
-60
-72
$\frac{\Delta I}{I_o}\Big)_{333}$ (%)
.40
.80
FLUENCE (10^{18} e/cm^2)
0
100
200
300
ANNEALING TEMP. (°K)
$\frac{\Delta I}{I}$
$\Delta\rho$
0
8
16
24
32
40
48
$\Delta\rho(10^{-10}\,\Omega\,cm)$

Using a total displacement cross section of 127 barns for 3 MeV electrons on copper,[20] and assuming simple production rate as given by:

Concentration of defects = (total cross section for production per electron) × (total number of electrons)

$$C_i = \sigma_T \phi \qquad (2)$$

σ_T = 127 barns

ϕ = fluence (electrons per cm^2) ,

we get a concentration of

$$C_i = (127 \times 10^{-24} cm^2)(.208 \times 10^{18} e/cm^2) = .264 \times 10^{-4} .$$

With a resistivity change of $\Delta\rho$ for this number of defects, the resistivity per atomic percent of defects, $\Delta\rho/1\%$, is given by

$$\Delta\rho = \Delta\rho/1\% \times C_i \text{ (in \%)}$$

$$\Delta\rho/1\% = \frac{22.8 \times 10^{-10}\ \Omega\text{-cm}}{.264 \times 10^{-2}\ (\%)} = .86\ \mu\Omega\text{-cm/\%} .$$

The four values of resistivity change per atomic percent of defects are .695, .817, .863, and .902 μΩ-cm/atomic %. The average of the last three values is .857 μΩ-cm/atomic %. Two previous irradiations of about the same fluence without the x-ray crystals yielded resistivity changes equal to the above average ± 10%.

These values are to be compared with data of Corbett et al.[22] Their source of high energy electrons produced an electron beam with a gated half sine wave of voltage, the average energy of which was 1.37 MeV. Various problems associated with beam measurement and uncertainty

in the exact position of the sample during irradiation introduced a ± 10% uncertainty in their fluence measurement. Using a threshold displacement energy of 22 eV, the value for the total displacement cross section at 1.37 MeV is σ_T = 70 barns.[20] It should be noted that further error is introduced since for their non-constant voltage, $\sigma_T(\overline{E})$ does not necessarily equal $\overline{\sigma_T(E)}$. A typical set of data are

$$\Delta\rho = 2.06 \times 10^{-10}\ \Omega\text{-cm}$$

$$\phi = 2.56 \times 10^{16}\ \text{elec/cm}^2 .$$

This yields a value of $\Delta\rho/\% = 1.15\ \mu\Omega$-cm. The rest of their data yield values between 1.14 and 1.19 μΩ-cm. The value of .86 μΩ-cm represents an error of 25% from the average Corbett value.

The fluence measurement uncertainty in this experiment is less than or equal to the 10% error in the Corbett measurement. His use of the value 3.93×10^{-3}/degree C for the resistivity temperature coefficient will result in a small error. There is probably a large error introduced in comparing resistivity changes from electrons differing in energy by greater than a factor of two. The determination of the cross section is highly dependent on the threshold energy which is not accurately known[24,25] and which is different for different recoil directions. The energy loss of the primary displaced atoms is not well known and, therefore, the number of secondary displacements is not accurately known. An illustration of the problem with total cross section determination is the use by Corbett *et al.* of σ_T = (57 ± 17) barns which differs considerably from the more recently calculated value of 70 barns of Oen.

In view of these problems, the value of resistivity change per atomic % of defects is acceptable, and the primary purposes of the resistivity measurements -- uniform fluence check, irradiation temperature and annealing effects -- are achieved.

The x-ray intensity data show different behavior from the resistance data. The main features can be represented by the following points:

1. The intensity changes for (111), (222), (333), and (220) are larger than predicted by the theoretical concentration of point defects,[11] whereas the changes for the (200) and (400) reflections are in the predicted range.

2. In Run I the intensity decrease was quadratic with fluence as contrasted with the linear behavior of the resistance changes.

3. Run II, which used the same x-ray crystals as Run I after a three-month room temperature anneal, shows a similar quadratic production rate and exhibits a production rate of approximately twice that of Run I.

4. In both runs the x-ray intensity showed almost full recovery after Stage I annealing (our 78 K anneal).

DISCUSSION

There are three remarkable features of the anomalous transmission data. The decreases in x-ray intensity are not linear with electron fluence. Second, electron irradiation at 14 K plus a long anneal at 295 K leaves the specimen in an altered state such that a subsequent low temperature electron irradiation produces larger x-ray intensity decreases than occurred during the first irradiation -- a "radiation history" effect. Third, the decrease in intensity for the (nnn) planes vary more rapidly than n^2. At present we do not have an understanding of these results.

As mentioned previously, the resistivity data have been used to establish the accuracy of the fluence measurements and irradiation temperature. These facts will be assumed to apply to the x-ray crystals as various models are considered. The important differences between the resistivity data and the x-ray data should be clearly emphasized. The two properties were measured on different samples that were prepared differently. As pointed out in the Introduction, x-ray anomalous transmission is much more sensitive to strain and defect clustering than is resistivity. The resistivity data may not, therefore, be a measure of defect behavior in the x-ray crystals, but rather act as a check on the electron beam measurement.

If the production of defects is linear with electron fluence as seen by the resistivity measurements and as expressed by equation (2), then then non-linear change in x-ray intensity requires the intensity to have a greater than linear dependence on defect concentration. The concen-

tration dependence was investigated by calculating the absorption coefficient due to irradiation μ^*

$$I = I_o e^{-\mu^* t} \tag{3}$$

with I and I_o as in equation (1) and t the sample thickness. $\mu^* t$ was calculated for all planes after the various values of electron fluence. The ratio of $\mu^* t$ for full fluence to half fluence was $4.1 \pm .3$ in Run I and $3.9 \pm .4$ in Run II. Quadratic dependence of μ^* on fluence predicts a value of $(2)^2 = 4$. Therefore, experimentally we see

$$\mu^* = A\phi^2 \tag{4}$$

where A is a constant depending on the reflecting planes considered and ϕ is the electron fluence. Figure 15 is a plot of $\mu^* t$ vs. ϕ^2. If

$$C_i = \sigma_T \phi \tag{2}$$

then

$$\mu^* = A\left(\frac{C_i}{\sigma_T}\right)^2 = A' C_i^2 . \tag{5}$$

The effective absorption coefficient is then quadratically proportional to the defect concentration.

The annealing data were inspected assuming quadratic dependence on concentration for the absorption coefficient. The x-ray intensity change can then be found from (1)

$$\frac{\Delta I}{I_o} = \frac{I_o - I}{I_o} = \frac{I_o - I_o e^{-\mu^* t}}{I_o} = 1 - e^{-\mu^* t} = 1 - e^{-A' C^2 t} . \tag{6}$$

The percentage of the initial defect concentration remaining after an anneal was taken from the electrical resistivity recovery data assuming

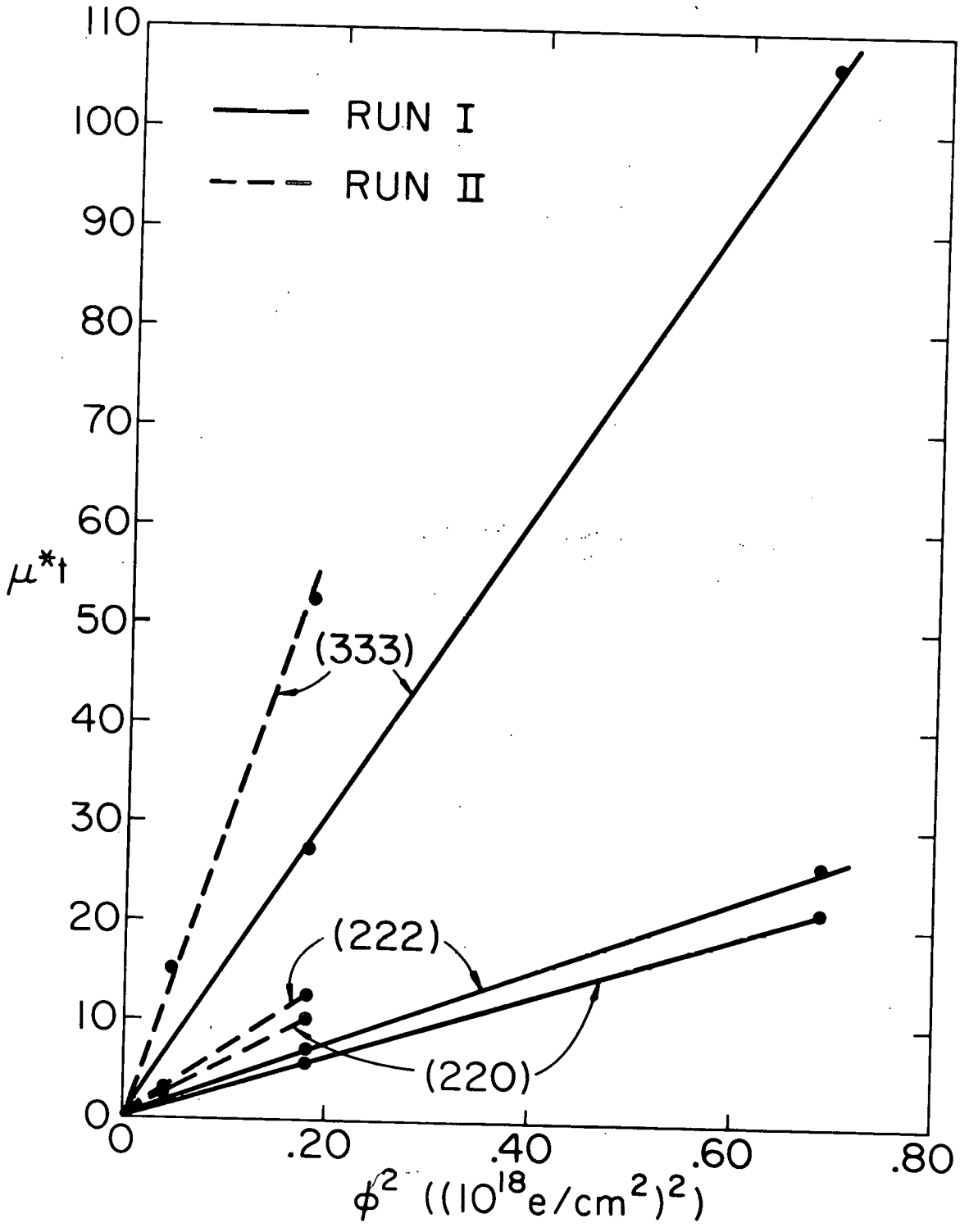
110
100
90
80
70
60
50
40
30
20
10
0
μ*t
RUN I
RUN II
(333)
(222)
(220)
0
.20
.40
.60
.80
φ² ((10¹⁸e/cm²)²)

an x% recovery in resistivity resulted from an x% annihilation of defects. This assumes that all defects that recover at different temperatures have the same resistivity, and application of the recovery idea to the x-ray crystal represents an additional assumption. The recovery after the 22 K anneal was too small to be analyzed.

Table 4 shows the predicted and observed recovery. The agreement appears good and gives additional evidence of the quadratic dependence for μ^* as observed experimentally during irradiation.

Table 4

X-Ray Intensity Recovery After Annealing

	PREDICTED			OBSERVED		
	After 37 K	After 77 K	After 295 K	After 37 K	After 77 K	After 295 K
222	75%	97%	99%	71%	97%	99%
333	67%	96%	99%	63%	93%	99%
220	75%	98%	99%	69%	98%	99%

The possibility of quadratic dependence of the defect concentration on electron fluence, and linear dependence of the absorption coefficient on concentration has not been overlooked. In view of the linearly observed production rate for resistivity and the previously observed linearity, this possibility seems less likely than the above model. Assuming the first model it is necessary to understand the non-linear decrease of x-ray intensity resulting from a linear production of defects. Possible examples of such a mechanism are straining of the reflecting atomic planes or clustering of the defects.

The influence of long range strain on the reflecting atomic planes was investigated using a theory developed by Okkerse and Penning.[12] They give expressions for the anomalously transmitted and reflected beams for deformed perfect crystals when the strain extends over distances large compared to an extinction distance. (An extinction distance is the distance required to obtain the standing waves appropriate for anomalous transmission. In copper for Mo K_α it is 10^{-4} cm.) An undeformed crystal should have the same x-ray intensity for (hkl) and $(\bar{h}\bar{k}\bar{l})$ reflections. Only certain kinds of strains can be detected by the intensity difference between the (hkl) and $(\bar{h}\bar{k}\bar{l})$ reflections. Given the geometry of the crystal and the irradiation, symmetry arguments yield a strain model that could be used in the Penning theory. It is not to be assumed that this strain model is the only one that could be used. This expression for the strain from the difference of the (hkl) and $(\bar{h}\bar{k}\bar{l})$ reflections can then be used in the average of the front and back reflections to give an estimate of the effect of long range strain. All of the intensity results use the average of the front and back reflections and the data show that for the (111), (222), and (220) reflecting planes the calculated change due to strain is less than 1% throughout both experimental runs, and changes in the strain contribution are much less than 1% for successive x-ray measurements during irradiation and annealing. The intensity change upon irradiation for the (222) and (220) planes is on the order of 20% and the calculated long range strain can account for 1% at most.

A general theory dealing with anomalous transmission of x-rays in strained perfect crystals has not been satisfactorily completed. Penning discusses in considerable detail the dynamical theory of x-ray diffraction

and its application to strained crystals.[26] He derives a ray theory for slightly deformed crystals. Penning discusses only cases in which the deformation varies slowly, i.e. $\Delta u/u$ is small compared with unity where Δu is the change in the atomic displacement as one traverses an extinction distance. The basic assumption is that in deformed crystals well defined beams are present as in undeformed crystals. Thus, his theory may be applied only if the strain is not too inhomogeneous. It is assumed that for slowly varying strain, "one mode remains one mode." The adjustment of the wave field to the gradually changing lattice requires only a gradual change in wave vector and amplitude. The absence of generated modes with an appreciably different wave vector puts an upper limit on the permissible change in reciprocal-lattice vector per unit distance. Penning treats in an exact form without using the above assumptions of the ray theory only some particularly simple and highly symmetric strains. The strain is a linear function of one space coordinate only. From the exact treatment for simple examples it follows that for sufficiently slowly varying strain the ray theory gives correct results.

It has been established experimentally[3,7,9] and theoretically that the aggregation of defects into clusters or loops has a much larger effect on the absorption of anomalously transmitted x-rays than do the same number of isolated point defects. An attempt has been made to fit the theory of Dederichs[10] to our data. Using the parameter $H = 2\pi/d_{hkl} = (2\pi/d)(h^2+k^2+1^2)^{1/2}$ to characterize the reflecting planes, the theory predicts an H dependence for the photoelectric absorption coefficient of $H^{3/2}$ for loops and H^2 for spherical clusters. The absorption coefficient, μ^*, is defined in equation (3). Figure 16 is a plot of $\mu^* t$ vs. H for

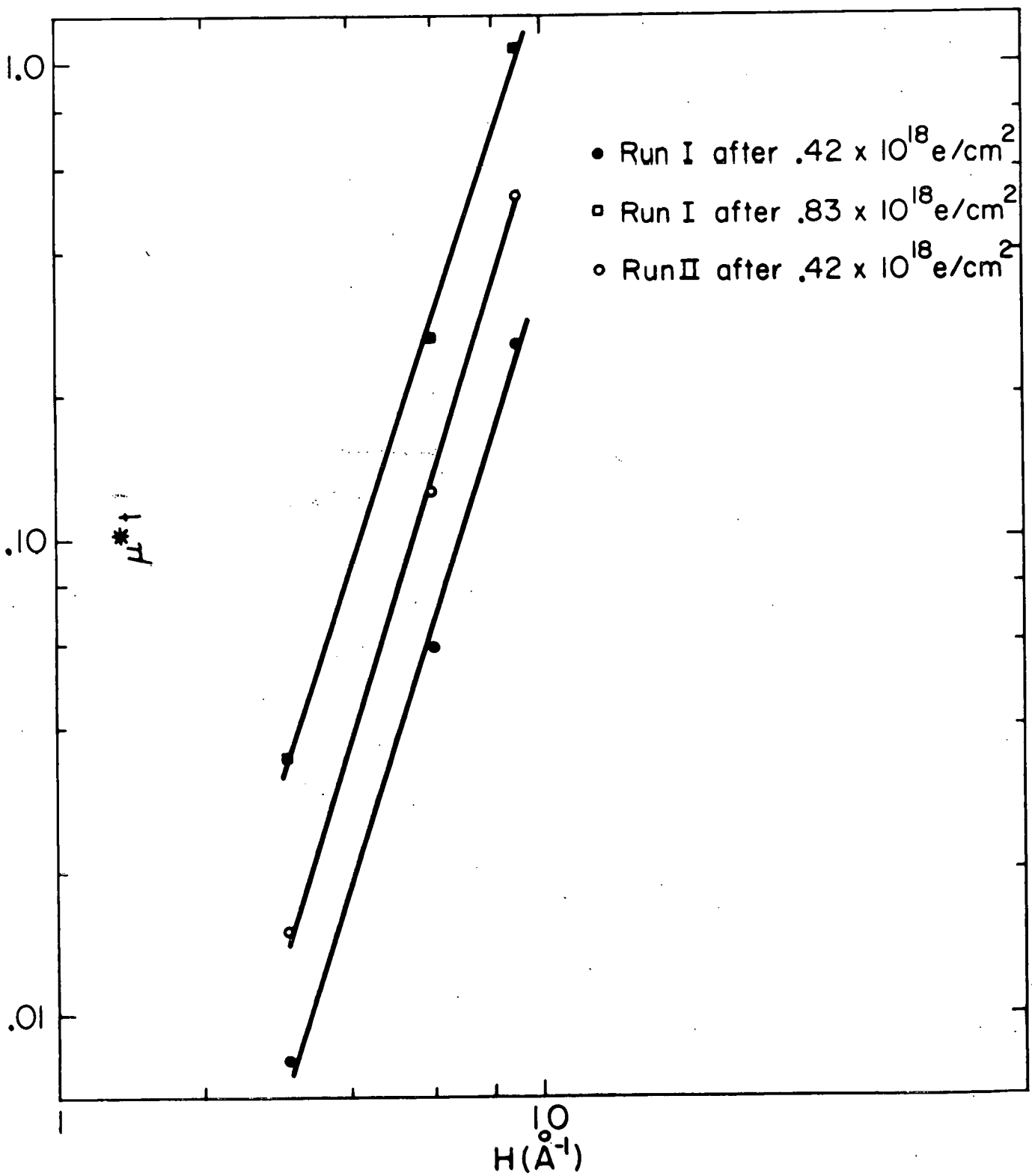
1.0
.10
.01
$\mu^*\uparrow$
1
10
H(Å^{-1})
• Run I after .42 x 10^{18} e/cm^2
▫ Run I after .83 x 10^{18} e/cm^2
◦ RunII after .42 x 10^{18} e/cm^2

both runs. The three nearly parallel straight lines have a slope of $3.1 \pm .2$. This is larger than the 2 or 3/2 slope predicted for photoelectric absorption. It should be mentioned that the H^2 dependence for μ^*_{PE} (clusters) is the first term of an expansion in H^2. Calculations have shown that the H^4 term contribution to μ^*_{PE} (clusters) is less than 10% of the H^2 term and is insufficient to increase the H dependence significantly above H^2.

Dederichs points out that the diffuse scattering absorption coefficient, μ_{DS}, is even more sensitive to clustering than is the photoelectric absorption coefficient, μ_{PE}. Estimated loop radii were found by assuming $\mu_{PE} >> \mu_{DS}$. These radii were then put in Dederichs theory for μ_{DS}. It was found that $\mu_{DS} < .01\,\mu_{PE}$ for all planes and it appears that the estimated cluster radii are too small to give significant diffuse scattering.

Dederichs' theory is a generalization of the dynamical theory which considers only the mean elastic or coherent wave, the scattering of which can be described by an effective periodic potential. He applies the theory to statistically distributed defect aggregates, the sizes of which are small compared with an extinction length. It is assumed that the measured intensity does not depend on the accidental microscopic defect configuration in a given crystal, but only on macroscopic quantities as the average defect density. Attention is restricted to the coherent wave, that part of the total wave which interferes with the incident wave, since for small defect clusters the other parts of the total waves, the diffuse waves, do not satisfy the Bragg condition due to oblique angle scattering and are absorbed in the crystal in the normal way.

The displacement fields of defect aggregates must be known in order to understand the effect of clustering on photoelectric absorption. Because calculations from first principles are not available, Dederichs considers two models -- loose clusters with spherical symmetry and disks of defects or dislocation loops. The displacement fields are found assuming a continuum theory displacement field for a single point defect and appropriately summing these displacements, resulting in displacements of all defects in the same cluster adding coherently and different clusters adding incoherently. The cluster model assumes the defects in the cluster are independently distributed and have a constant defect density. The loop model assumes a distribution of loops over all equivalent cubic directions, resulting in a loss of sensitivity of the incident x-ray beam direction.

The purpose of this brief discussion of Dederichs' theory is to understand upon what assumptions the theory is based. His assumptions of statistically distributed clusters or loops, distribution of loop orientations, and constant defect density in the clusters may not be valid in the case of defect aggregation in our specimens. The crystals used in the present experiments were irradiated with 10^{17} fast n/cm^2 at 100 C to pin existing dislocations, thus hardening the crystals. Various estimates have been made as to the effect of this n irradiation on the crystals,[17] but it can be assumed that this 100 C irradiation results in the production of some damage, probably in the form of defect aggregates. Topographs of the crystal show no dislocations passing through the crystal and very few aggregates as large as 5 μ in diameter. Although our crystals appear to be nearly perfect with respect to x-ray diffraction

properties;[18] the presence of this damage could affect subsequent defect aggregation upon electron irradiation. An example of this would be the migration of interstitials away from regions of increased strain around interstitial loops. The presence of the neutron damage will probably upset the statistical distributions assumed by Dederichs, and the effect of this on expressions for the absorption coefficients has not been determined.

Topographs were taken of our crystal before any electron irradiation and after Run II. No new defect clusters $\gtrsim 5\ \mu$ in diameter could be seen in the post-irradiation topographs. The topographs were taken after Run II to see if any large clustering had occurred, but there was essentially no difference in the two sets of topographs.

The intensity changes for the (200) and (400) reflecting planes are considerably smaller than the other planes. This can be the result of an anisotropic effect where the displacements normal to the (200) planes are less than the displacements normal to the (111) and (220) planes. The anisotropic stress field produced by a point force in a cubic crystal has been calculated.[27] The displacement of an atom a distance r from a point force goes as $1/r^2$. For copper the anisotropic theory yields that the displacement perpendicular to the (111) plane is 7 times the displacement perpendicular to the (100) plane. The displacement perpendicular to the (110) plane is 5 times the displacement perpendicular to the (100) plane. These calculations are useful for atoms greater than a few atomic distances from the point force. Thus, if the long range displacements are important, anisotropy plays a very important role in atomic displacements. There is no complete discussion of the relative role of displace-

ments for atoms a few atomic distances of less from the force and for atoms at a greater distance.

The radiation history effect indicates that different mechanisms are observed in the resistivity and x-ray samples. The changes in x-ray intensity, but not resistivity (measured on different specimens), are larger on a second electron irradiation at low temperature after a three month 295 K anneal than the changes during the initial 14 K irradiation. The x-ray changes show more than 90% recovery after a 77 K anneal and nearly full recovery after the 295 K anneal. Thus, the history effect does not decrease the intensity after annealing, but does leave the specimen in a state resulting in enhanced defect production upon subsequent irradiation. The present crystal received an irradiation of $.4 \times 10^{18}$ e/cm^2 prior to the first reported irradiation. The results of this irradiation could not be measured due to equipment failure. This crystal was used for subsequent irradiations since the radiation history effect was not known until two full irradiations later. This previous unreported irradiation and the observed importance of radiation history are important in comparing the present x-ray data with that previously reported by Edelheit, et al.[11] His 22 K irradiation on a previously unirradiated crystal resulted in intensity changes considerably smaller than reported here.

As mentioned previously, the crystals were hardened by neutron irradiation. This introduced a number of small defect loops or clusters. It was mentioned how such loops could affect the defect production. If upon annealing the number and size of these loops changes so that there are a greater number of loops, it is then possible that the production rate upon irradiating this sample with a new loop distribution would be larger.

Any model such as this must incorporate the fact that we see nearly full intensity recovery after annealing and, therefore, an increase in the number of loops requires an appropriate decrease in their size to permit the x-ray intensity to recover to its initial value. This model is presented qualitatively only since quantitative analysis requires further experimentation, possibly electron microscopy.

CONCLUSIONS

The anomalous x-ray transmission experiments were initiated to determine the structure of the interstitial in copper. Unfortunately, the interpretation of the experiments is clearly more complex than originally expected. The three remarkable observations described above cannot at this point be understood in terms of any existing theory.

In view of the fact that none of the existing models answers all of the questions posed by the data, thought has been given to future experiments. The non-linear intensity decrease could be investigated by simultaneously measuring on the same specimen the electrical resistivity or lattice parameter together with anomalous transmission intensity. If, as suspected, small defect clusters are responsible for the "radiation history" effect, it may be necessary to inspect the crystals with the electron microscope. Lattice parameter measurements might reveal that some alteration of the crystals had occurred, but would not give unequivocal knowledge as to the actual crystallographic process. None of the existing theories gives the very large observed dependence on H for the absorption coefficient. Measurements of the intensity change for different wavelengths can give a measure as to the relative importance of photoelectric absorption and diffuse scattering. The importance of multiple knock-ons from the 3 MeV electrons could be investigated by using lower energy electrons. The effect of cluster formation on the radiation history could be studied by a high temperature anneal of the samples between irradiations.

LIST OF REFERENCES

1. B. W. Batterman and H. Cole, Rev. of Mod. Phys. 36, 681 (1964).
2. R. W. James, Solid State Physics, Vol. 15, p. 53, F. Seitz and D. Turnbull, eds. (Academic Press, Inc., New York, 1963).
3. J. R. Pattel and B. W. Batterman, J. Appl. Phys. 34, 2716 (1963).
4. O. N. Efimov, E. G. Sheikhet, and L. I. Datsenko, Phys. Status Solidi 38, 489 (1970).
5. R. Collella and A. Merlini, Phys. Stat. Sol. 14, 81 (1966).
6. T. O. Baldwin and J. E. Thomas, J. Appl. Phys. 39, 4391 (1968).
7. T. O. Baldwin, F. A. Sherrill, and F. W. Young, Jr., J. Appl. Phys. 39, 1541 (1968).
8. F. W. Young, Jr., T. O. Baldwin, and P. H. Dederichs, in Vacancies and Interstitials in Metals, edited by A. Seeger, D. Schumacher, W. Schilling, and J. Diehl (North-Holland, Amsterdam, 1970).
9. B. C. Larson and F. W. Young, Jr., Phys. Rev. B 4, 1709 (1971).
10. P. H. Dederichs, Phys. Rev. B 1, 1306 (1970).
11. L. S. Edelheit, J. C. North, J. G. Ring, J. S. Koehler, F. W. Young, Jr., Phys. Rev. B 2, 2913 (1970).
12. B. Okkerse and P. Penning, Phillips Res. Rept. 18, 82 (1963).
13. P. Penning and D. Polder, Phillips Res. Rept. 16, 419 (1961).
14. For a discussion, see J. W. Corbett, in Solid State Physics, edited by F. Seitz and D. Turnbull (Academic Press, New York, 1966), Suppl. 7.
15. F. W. Young, Jr. and J. R. Savage, J. Appl. Phys. 35, 1917 (1964).
16. F. W. Young, Jr. and T. R. Wilson, Rev. Sci. Instr. 32, 559 (1961).
17. R. M. Nicklow, F. A. Sherrill, and F. W. Young, Jr., Phys. Rev. 137, A1417 (1965).
18. T. O. Baldwin, F. W. Young, Jr., and A. Merlini, Phys. Rev. 163, 591 (1967).
19. E. H. Sondheimer, Advances in Physics 1, 1 (1952).
20. O. S. Oen, ORNL Report No. ORNL-3813, 1965 (unpublished).

21. A. V. Granato and T. G. Nilan, Phys. Rev. 137. A1250 (1965).

22. J. W. Corbett, J. M. Denney, M. O. Fiske, and R. M. Walker, Phys. Rev. 108, 954 (1957).

23. A. N. Gerritsen, Handbuch der Physik, Vol. XIX, p. 137 (1956).

24. G. W. Iseler, H. I. Dawson, A. S. Mehener, J. W. Kauffman, Phys. Rev. 146, 468 (1966).

25. W. Bauer and A. Sosin, J. Appl. Phys. 37, 1780 (1966).

26. P. Penning, Phillips Res. Rept., Supp 5 (1965).

27. K. Lie and J. S. Koehler, Advances in Physics 17, 421 (1968).

Percentage Decrease in Transmitted X-ray Intensity $\frac{\Delta I}{I_o}$ for (hkℓ) and ($\bar{h}\bar{k}\bar{\ell}$)

RUN I

Reflecting Planes	After 1/2 fluence			After total fluence			After 22 K Anneal			After 37 K Anneal			After 77 K Anneal			After 295 K Anneal		
	(hkℓ)	($\bar{h}\bar{k}\bar{\ell}$)	Ave.	(hkℓ)	($\bar{h}\bar{k}\bar{\ell}$)	Ave.	(hkℓ)	($\bar{h}\bar{k}\bar{\ell}$)	Ave.	(hkℓ)	($\bar{h}\bar{k}\bar{\ell}$)	Ave.	(hkℓ)	($\bar{h}\bar{k}\bar{\ell}$)	Ave.	(hkℓ)	($\bar{h}\bar{k}\bar{\ell}$)	Ave.
111-1	.4	1.2	.8	2.3	4.5	3.4	2.3	4.5	3.4	.4	1.4	.9	.1	.5	.3	0.0	.4	.2
111-2	4.0	7.6	5.8	19.7	26.7	23.2	19.5	26.5	23.0	4.3	9.3	6.8	0.2	1.0	.6	0.0	.4	.2
111-3†	14.9	30.7	22.8	57.3	74.1	65.7	57.2	74.0	65.6	18.6	30.0	24.3	4.0	4.8	4.4	0.0	.2	.1
220-1	3.9	6.9	5.4	16.8	22.0	19.4	16.7	21.7	19.2	4.1	7.9	6.0	.1	.3	.2	0.0	.2	.1
200-1				.3	.5	.4										.1	.3	.4
200-2				1.2	2.0	1.6										.4	*	.4

RUN II

Reflecting Planes	After 1/8 fluence			After 1/4 fluence			After 1/2 fluence		
	(hkℓ)	($\bar{h}\bar{k}\bar{\ell}$)	Ave.	(hkℓ)	($\bar{h}\bar{k}\bar{\ell}$)	Ave.	(hkℓ)	($\bar{h}\bar{k}\bar{\ell}$)	Ave.
111-1							*	1.5	1.5
111-2	.6	.4	.5	3.4	2.4	2.9	12.7	10.9	11.8
111-3†	2.6	3.2	2.9	13.3	14.5	13.9	40.3	41.3	40.8
220-1	.3	.5	.4	2.2	2.6	2.4	9.4	9.8	9.6

†(hkℓ) and (hkℓ) were taken at different locations for 111-3 reflection for both runs.
*data not available.

VITA

Bruce Stilwell Brown was [redacted]

He attended Sutherland elementary school and Morgan Park High School in Chicago.

He received a B.A. degree in Applied Mathematics (with high honors) at Miami University in April, 1966. He entered the Graduate College, University of Illinois in September, 1966, and received an M.S. degree in Physics in February, 1968.

He held a teaching assistantship (1967-68) and a research assistantship (1968-72) while at the University of Illinois.

He is a member of the American Physical Society and Phi Beta Kappa.